Cell Reports

Article

FOXO1 constrains activation and regulates senescence in CD8 T cells

Graphical Abstract

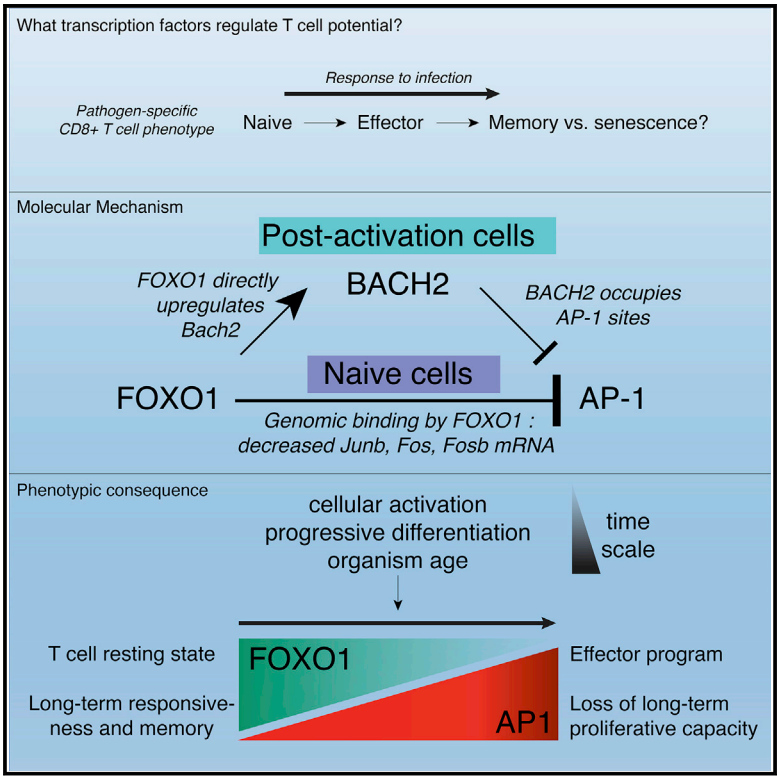

Highlights

- FOXO1 opposes senescence and the effector program in T cells
- FOXO1 directly binds genomic loci of AP-1 subunits and AP-1 repressor BACH2
- Age and progressive cellular differentiation each decrease FOXO1 and increase AP-1

Authors

Arnaud Delpoux, Nimi Marcel, Rodrigo Hess Michelini, ..., Martha Lappas, Stephen M. Hedrick, Andrew L. Doedens

Correspondence

shedrick@ucsd.edu (S.M.H.), adoedens@gmail.com (A.L.D.)

In Brief

Delpoux et al. find that FOXO1 maintains T cells in a resting state, with greater differentiation and proliferative capacity, in part by attenuating AP-1. In humans, T cell differentiation and aging result in lower FOXO1 and characteristics of senescence. These findings place FOXO1 as a key negative regulator, counter to senescence, in T cells.

Delpoux et al., 2021, Cell Reports *34*, 108674
January 26, 2021
https://doi.org/10.1016/j.celrep.2020.108674

Cell Reports

CellPress
OPEN ACCESS

Article

FOXO1 constrains activation and regulates senescence in CD8 T cells

Arnaud Delpoux,[1,2,5] Nimi Marcel,[1,2] Rodrigo Hess Michelini,[1,2] Carol D. Katayama,[1,2] Karmel A. Allison,[2] Christopher K. Glass,[2] Sergio M. Quiñones-Parra,[1] Cornelis Murre,[1] Liyen Loh,[3] Katherine Kedzierska,[3] Martha Lappas,[4] Stephen M. Hedrick,[1,2,6,*] and Andrew L. Doedens[1,2,*]

[1]Division of Biological Sciences, Molecular Biology Section, University of California, San Diego, 9500 Gilman Drive, La Jolla, CA 92093-0377, USA

[2]Department of Cellular and Molecular Medicine, University of California, San Diego, 9500 Gilman Drive, La Jolla, CA 92093-0377, USA

[3]Department of Microbiology and Immunology, University of Melbourne, Peter Doherty Institute for Infection and Immunity, Parkville, VIC, Australia

[4]Obstetrics, Nutrition, and Endocrinology Group, Department of Obstetrics & Gynaecology, University of Melbourne, Mercy Hospital for Women, Heidelberg, VIC, Australia

[5]Deceased

[6]Lead contact

*Correspondence: shedrick@ucsd.edu (S.M.H.), adoedens@gmail.com (A.L.D.)

https://doi.org/10.1016/j.celrep.2020.108674

SUMMARY

Naive and memory T cells are maintained in a quiescent state, yet capable of rapid response and differentiation to antigen challenge via molecular mechanisms that are not fully understood. In naive cells, the deletion of *Foxo1* following thymic development results in the increased expression of multiple AP-1 family members, rendering T cells less able to respond to antigenic challenge. Similarly, in the absence of FOXO1, post-infection memory T cells exhibit the characteristics of extended activation and senescence. Age-based analysis of human peripheral T cells reveals that levels of FOXO1 and its downstream target, TCF7, are inversely related to host age, whereas the opposite is found for AP-1 factors. These characteristics of aging also correlate with the formation of T cells manifesting features of cellular senescence. Our work illustrates a role for FOXO1 in the active maintenance of stem-like properties in T cells at the timescales of acute infection and organismal life span.

INTRODUCTION

Relative to stem cells, newly formed T cells are highly differentiated, yet maintain the qualities of self-renewal, an ability to repeatedly enter and exit the cell cycle, and plasticity with regard to further differentiation. These properties contribute to the continuing ability of a host to attain adaptive immunity to novel pathogens, and at the same time to maintain a large repertoire of T cells that can serially or continually respond to persistent infections. With age, however, naive and memory T cells shift to a more differentiated state, and take on a senescent phenotype that restricts their ability to respond to an antigenic stimulus and proliferate without a loss of viability (Goronzy and Weyand, 2017; Gustafson et al., 2018). The molecular mechanisms governing T cell self-renewal, differentiation capacity, and the changes observed in aged individuals are not fully understood.

The FOXO family of transcription factors display pro-longevity characteristics first discovered in genetic screens of *Caenorhabditis elegans* (Kenyon et al., 1993; Gottlieb and Ruvkun, 1994). These features extend across phyla, as FOXO1 and FOXO3 polymorphisms are linked to exceptional longevity in multiple human populations throughout the world (Lunetta et al., 2007; Li et al., 2009; Kenyon, 2010). The basis for this is likely to be complex, but one relevant aspect may be a role for FOXO1 in the active suppression of cellular differentiation. This has been shown for pluripotent human and mouse embryonic stem cells (Zhang et al., 2011) and organ-specific stem cells with more limited differentiation potential (Liang and Ghaffari, 2018; McLaughlin and Broihier, 2018). For lymphocytes, FOXO1 is essential for the induction of memory T cells capable of self-renewal and re-expansion in response to antigenic stimulation (Rao et al., 2012; Hess Michelini et al., 2013; Kim et al., 2013; Tejera et al., 2013), as it promotes the partitioning of memory and effector subsets within days of a viral infection (Delpoux et al., 2017). It is furthermore necessary for the maintenance of a memory state in T cells poised to respond to antigen (Delpoux et al., 2018; Utzschneider et al., 2018). FOXO1 appears to be regulated, in part, as a target of miRNA regulation that correlates with altered naive T cell homeostasis during human aging (Gustafson et al., 2018).

Here, we show that FOXO1 actively maintains T cell quiescence and proliferative potential such that, in its absence, naive T cells upregulate a subset of post-activation effector transcripts such as *Ifng*. Initially, this correlated with the activation of the AP-1 family of transcription factors, heterodimeric complexes that bind to palindromic 12-*O*-tetradecanoylphorbol-13-acetate (TPA) response elements (TREs; 5′-TGA (C/G)

TCA-3′) (Turner and Tjian, 1989; Foletta et al., 1998; Shaulian and Karin, 2002); however, upon antigen-induced T cell activation, the regulation of AP-1 factors was found to be mechanistically transferred to the gene encoding BACH2, itself a direct target of FOXO1 (Roychoudhuri et al., 2016; Tamahara et al., 2017). These findings led us to an examination of human T cells partitioned by phenotype or age that followed a progression toward senescence, and this progression was closely correlated with the extent of FOXO1 expression and a direct target, *Tcf7*. We conclude that FOXO1 functions in T cells to actively prevent terminal differentiation and senescence, and it is essential to maintain the ability of T cells to effectively respond to primary or subsequent stimulation. We propose AP-1 inhibition as one of the intrinsic mechanisms by which FOXO1 attenuates effector programs and maintains T cell proliferation and differentiation capacities among antigen-specific T cells.

RESULTS

FOXO1 maintains quiescence in naive T cells

To determine how gene expression changes in naive cells with long-term *Foxo1* deletion, T cells from *Foxo1*$^{f/f}$ dLck-Cre (*Foxo1*-KO [knockout]) mice were compared with *Foxo1*$^{f/f}$ mice by RNA sequencing (RNA-seq) (Figure 1A). In dLck-Cre transgenic mice, CRE-recombinase (CRE) was shown to be expressed during thymus development subsequent to positive selection when CD3 is expressed at high levels and the thymocytes express either CD4 or CD8. In T cells found in the secondary lymphoid organs, CRE was shown to be expressed in >90% of mature CD8$^+$ T cells, but <75% of CD4$^+$ T cells (Zhang et al., 2005). Thus, in *Foxo1*-KO mice, *Foxo1* is deleted subsequent to thymic selection, and yet there are sufficient CD4$^+$ FOXO1$^+$ FOXP3$^+$ T cells to prevent spontaneous autoimmunity. The mice did not manifest any of the autoimmune characteristics of *Foxo1*$^{f/f}$ *Cd4*-Cre mice (Kerdiles et al., 2010). Genes that were more highly expressed in the wild-type (WT) versus *Foxo1*-KO cells in addition to *Foxo1* included *Il7r* (Kerdiles et al., 2009), *Klrd1* (CD94, known to be induced on activated CD8$^+$ T cells), and *Scarna2*, a LncRNA of unknown function (Zhang et al., 2019). However, the major effect observed in naive *Foxo1*-KO T cells was gene expression usually associated with T cell activation. Induced genes included *Nr4a1* (Nur77), *Egr1*, *Ccl5* (Rantes), and *Ifng*, but in addition, a number of genes encoding subunits of the complex AP-1 family, including *FosB*, *Fos*, *Jun*, *JunB*, *JunD*, and *Atf3* (Figure 1A).

These data imply that FOXO1 is required to maintain a quiescent state in naive T cells. To test for the regulation of FOXO1 before and during a viral infection, we analyzed the expression of total FOXO1 and a phosphorylated form of FOXO1 (S256 in human, S253 in mice) characteristic of exclusion from the nucleus (Calnan and Brunet, 2008). P14 T cells from naive mice, or mice that were infected with lymphocytic choriomeningitis virus-Armstrong (LCMV-ARM) for either 7 or 12 days were isolated and activated for various times in culture. The lysates were then analyzed for FOXO1, pFOXO1, and β-tubulin as a control (Figure S1). Naive T cells before activation strongly expressed FOXO1 in an unphosphorylated form, and with activation in culture, phosphorylation plateaued at approximately 30 min. As pFOXO1 increased, the total amount of FOXO1 decreased consistent with the well-established regulation of FOXO1 based on phosphorylation by AKT or SGK1 (Brunet et al., 2001; Guertin et al., 2006), resulting in nuclear export and degradation by 14-3-3 (Van Der Heide et al., 2004). LCMV-specific T cells isolated from mice infected for 7 days showed a similar, albeit exaggerated FOXO1 phosphorylation following activation in culture. From many previous studies (Kaech and Wherry, 2007), this population largely consists of cytotoxic effector cells. T cells from mice infected 12 days earlier displayed low amounts of FOXO1 that once again diminished with phosphorylation (Figure S1).

To verify that the differences in AP-1 gene expression were also reflected in protein expression, we analyzed the expression of FOS, JUNB, and FOSB in CD44^{low} (naive) and CD44^{high} (previously activated) T cells. For comparison, we analyzed mice in which FOXO1 is constitutively nuclear via the transgenic expression of a *Foxo1*-triple alanine phosphorylation mutant (*Foxo1*-AAA) (Burgering and Kops, 2002; Ouyang et al., 2012; Stone et al., 2015). Consistent with FOXO1 repression of AP-1 factor expression in naive T cells, we found FOS, JUNB, and FOSB to be relatively high in T cells from *Foxo1*-KO, intermediate in T cells from WT, and diminished in T cells from *Foxo1*-AAA mice (Figure 1B).

To explore direct FOXO1 regulation of AP-1 family genes, we performed chromatin immunoprecipitation sequencing (ChIP-seq) on chromatin bound by FOXO1 in naive P14 T cells from unimmunized mice, or P14 T cells harvested from host mice 12 days after infection with LCMV-ARM; also, we analyzed open chromatin in naive P14 and P14 T cells from LCMV-ARM-infected mice using assay for transposase-accessible chromatin using sequencing (ATAC-seq) (Buenrostro et al., 2013). The T cells were pre-sorted for KLRG1^{high} and KLRG1^{low} cells to segregate effector and memory-precursor populations. In both naive and post-infection (p.i.) T cells, among the prominent FOXO1-bound genomic sites were regulatory sequences of multiple AP-1 family members, including *Fos*, *JunB*, *FosB*, and *JunD* (Figure 1C). FOXO1 bound to open chromatin proximal to the transcription start site (TSS) of each of these genes, or to nearby presumed enhancers (e.g., upstream of *Fos*) (Figure 1C). Found for both naive and day 12 P14 T cells, these data are consistent with FOXO1 acting as a direct or indirect co-repressor for genes that mediate T cell activation and differentiation (Im and Rao, 2004; Li et al., 2012). Thus, T cells that undergo *Foxo1* gene deletion immediately following thymic development constitutively display some but not all characteristics of activation.

Recently activated *Foxo1*-KO T cells exhibit similar AP-1 subunit levels, but decreased BACH2

Foxo1-KO cells exhibit an increased activation phenotype after infection (Hess Michelini et al., 2013; Utzschneider et al., 2018). Given the similar genomic binding of FOXO1 to AP-1 family members at day 0 versus day 12 p.i., we anticipated that we would observe increased AP-1 factors following infection: our working hypothesis was that FOXO1 was acting as a direct transcriptional co-repressor of AP-1 subunits. Instead, we observed similar AP-1 subunit mRNA and protein abundance in both

CellPress
OPEN ACCESS

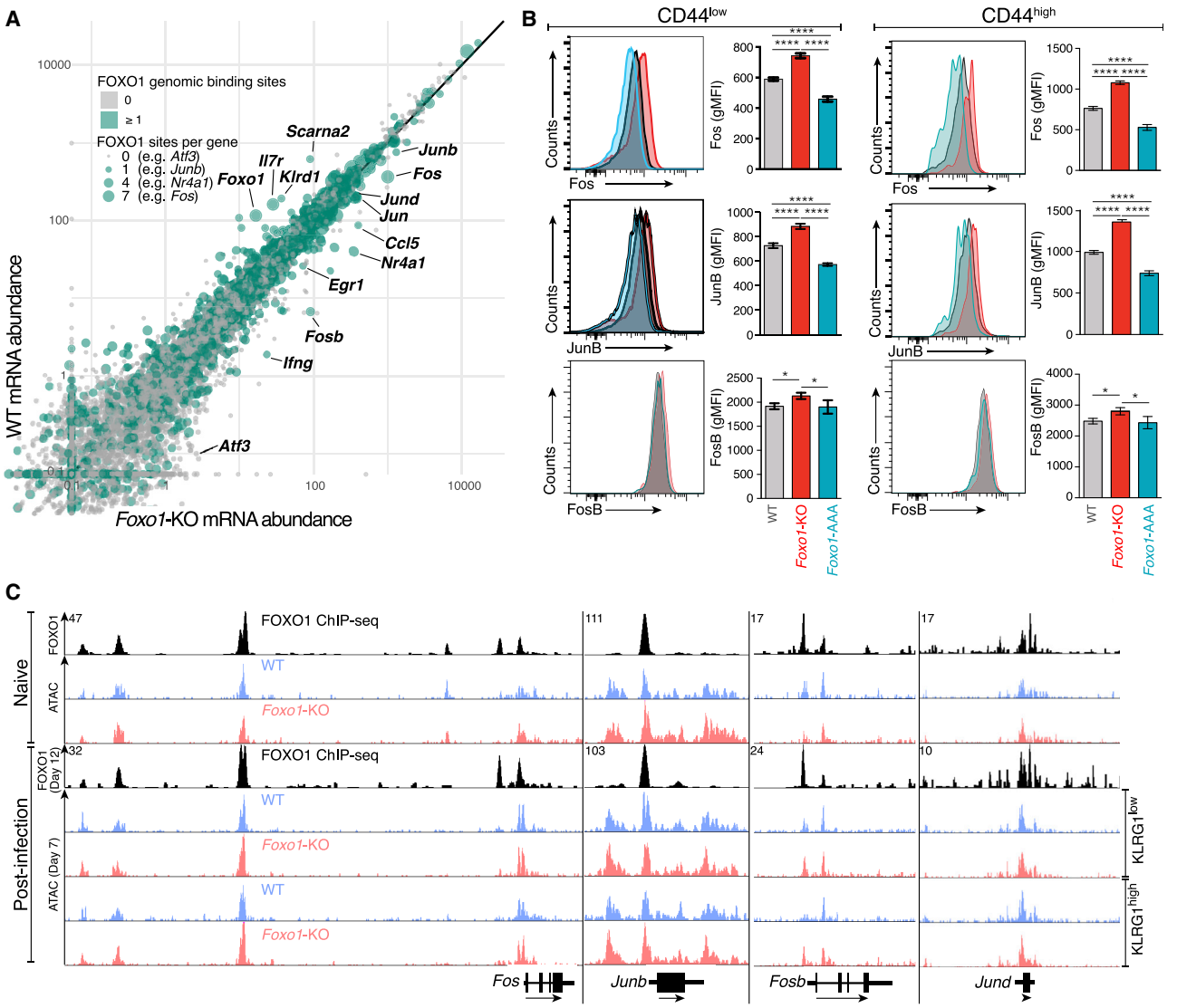

Figure 1. FOXO1 limits naive CD8$^+$ T cell AP-1 family member expression

(A) mRNA abundance (RNA-seq) of WT and *Foxo1*-KO naive CD8$^+$ T cells. Selected genes are labeled, including members of the AP-1 family. The gray point color indicates no FOXO1 genomic binding detected at day 0; green indicates ≥1 peaks detected; the size of points indicates the number of FOXO1 genomic binding sites nearest the gene TSS.

(B) Intracellular immunostaining determination of indicated protein abundance in naive P14 cells of the indicated genotypes and CD44 expression level.

(C) FOXO1 genomic binding (ChIP-seq) and chromatin accessibility (ATAC-seq) for select AP-1 subunits in naive and post-infection (p.i.) (LCMV-ARM) P14 T cells. The y-axis maximum for all ATAC-seq is 75.

For (B), data are averaged from 3 experiments with n = 3 mice per group per experiment. *p < 0.05; **p < 0.01; ***p < 0.001; ****p < 0.0001; unpaired Student's t test was used, and error bars represent means ± SEMs. Informatics experiments are from 1 biological sample per condition.

KLRG1^{low} and KLRG1^{high} P14 cells at 7 days post-activation (Figures 2A and S2A–S2D). Thus, FOXO1 does not directly regulate AP-1 subunit abundance at day 7 post-activation, despite detectable *Foxo1* mRNA (Figure S2E), and unambiguous genomic binding and regulation of known FOXO1 targets that include *Tcf7*, *Ccr7*, and *Sell* (Figures S2F and S2G).

A parallel molecular mechanism attenuating AP-1 activity is the BACH2 transcriptional repressor, a key regulator of quiescence. BACH2 binds to a subset of AP-1 sites, effectively blocking transactivation by AP-1 of proximal target genes (Roychoudhuri et al., 2016; Richer et al., 2016). We found that FOXO1 exhibited genomic binding within and proximal to the *Bach2* gene locus at multiple sites in naive and day 12 p.i. cells (Figure 2B). We observed that *Bach2* becomes FOXO1 dependent only post-activation. Whereas naive WT and *Foxo1*-KO cells had similar, abundant *Bach2* mRNA expression, 7 and 12 days post-activation WT cells exhibited a ~4-fold increase versus *Foxo1*-KO cells, in both KLRG1^{low} and KLRG1^{high} subsets (Figure 2C). As such, we predicted the target genes of AP-1 to be induced in BACH2-KO T cells.

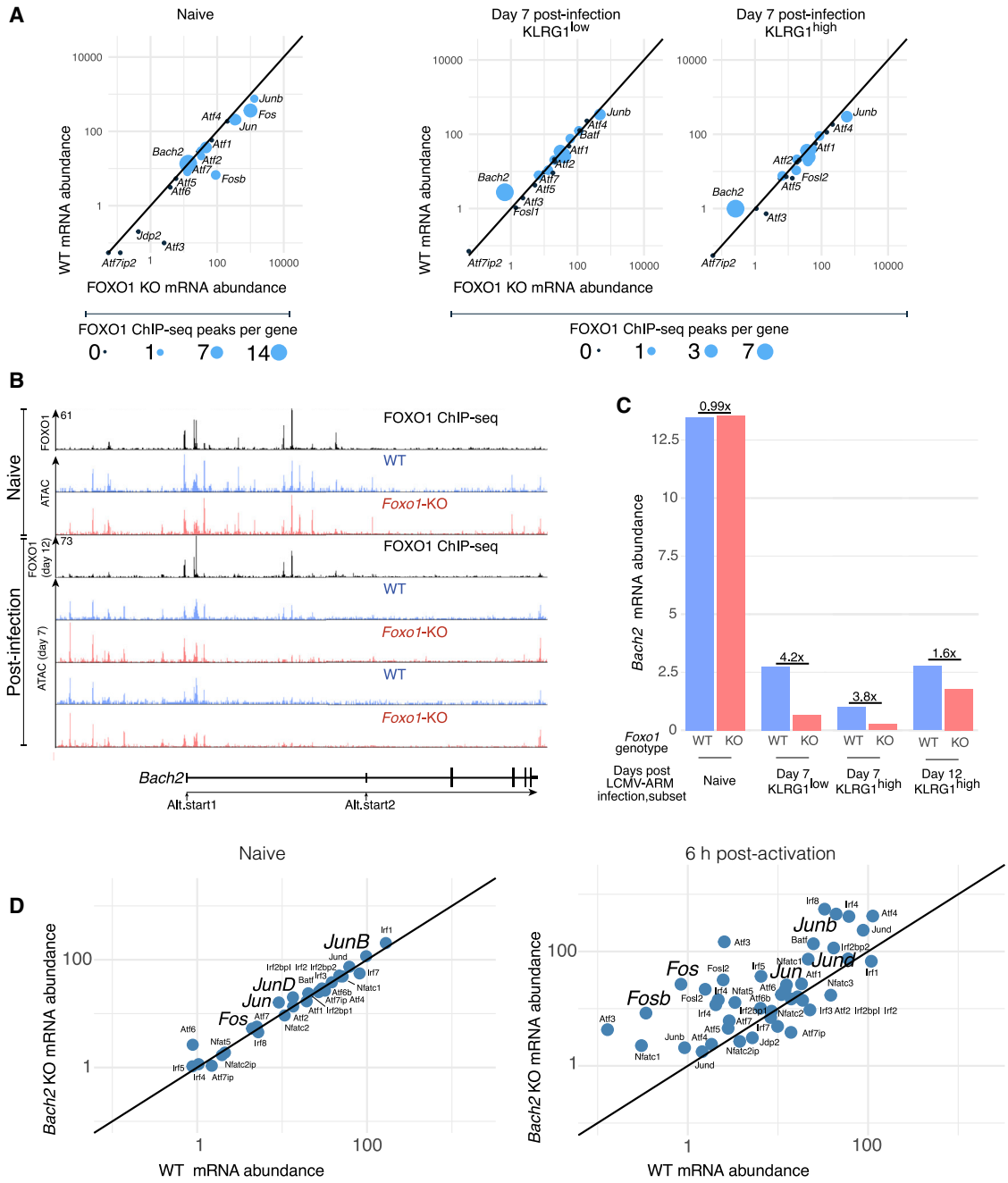

Figure 2. FOXO1 drives *Bach2* in post-activation CD8⁺ T cells to regulate AP-1

(A) Selected AP-1 family members RNA abundance from WT and *Foxo1*-KO naive CD8⁺ T cells at indicated time points, in uninfected mice or at indicated time/population p.i. with LCMV-ARM. Size of points indicates the number of FOXO1 genomic binding sites nearest the gene TSS.

(B) FOXO1 genomic binding (ChIP-seq) and chromatin accessibility (ATAC-seq) in naive and p.i. (LCMV-ARM) P14 T cells. All ATAC-seq y-axes maximums are 75.

(C) *Bach2* expression in WT and *Foxo1*-KO CD8⁺ T cells at indicated time points in naive or p.i. P14 cells.

(D) WT and *Bach2* KO cells before and after activation. (C and D: RNA-seq; primary data GEO: GSE77857).

The downstream activity of AP-1 homo- and heterodimers depends on the cell type and the exact AP-1 factors under analysis. Among myriad AP-1 targets, several are genes encoding subunits of the AP-1 factors themselves (Angel et al., 1988; van Dam et al., 1993; Gazon et al., 2018). To examine whether AP-1 target gene expression would respond to the deletion of the *Bach2* gene, we analyzed data comparing WT and *Bach2*-KO CD8⁺ naive and T cells activated for 6 h (Figure 2D; primary data from GEO: GSE77857; Roychoudhuri et al., 2016). In naive T cells, the family of AP-1 genes (including nuclear factor of

CellPress
OPEN ACCESS

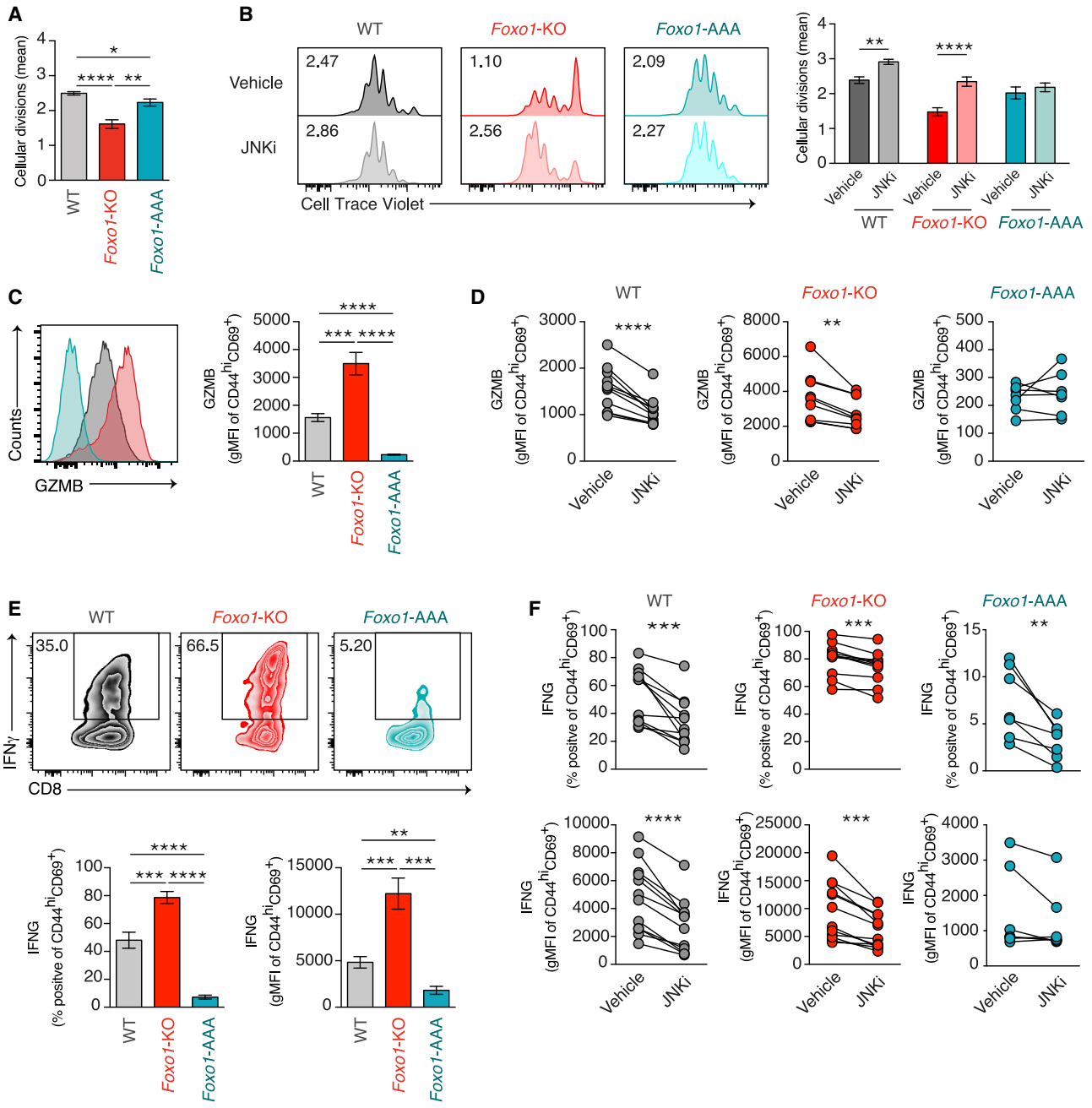

Figure 3. FOXO1- and JNK-dependent control of CD8$^+$ T cell effector functions and proliferation *in vitro*

(A–F) WT, *Foxo1*-KO, and *Foxo1*-AAA naive CD8$^+$ T cells were activated in culture through CD3 and CD28 and IL-2 for 3 days.

(A) Bar graph depicting the average number of cellular divisions of each genotype after 3 days.

(B) Histograms depicting the CellTrace Violet fluorescence for each genotype, with or without JNKi. The inset numbers represent the average number of cellular divisions. The bar graph (right) indicates the average number of cellular divisions for each genotype.

(C) GZMB intracellular immunostaining of CD8$^+$ T cells of the indicated genotypes. The bar graphs indicate the gMFI.

(D) GZMB expression in vehicle or JNKi-treated cells of the indicated genotypes.

(E) PMA/ionomycin (IONO) stimulation of cells of indicated genotypes followed by intracellular cytokine staining for IFN-γ. Bar plots represent percent of IFN-γ$^+$ among CD44hi CD69$^+$ cells (left panel) and gMFI of IFN-γ among IFN-γ$^+$ (right panel).

(F) IFN-γ expression following PMA/IONO re-stimulation with or without JNKi. Percentage of IFN-γ$^+$ among CD44^{hi} CD69$^+$ cells (upper panel) and gMFI of IFN-γ among IFN-γ$^+$ (lower panel).

(legend continued on next page)

activated T cell [NFAT] paralogs; Rao et al., 1997) were largely unaffected by the loss of *Bach2* (Figure 2D, left). In contrast, 6 h after activation, AP-1 family genes were strongly increased in *Bach2*-KO relative to WT T cells (Figure 2D, right). These observations are consistent with the idea that in the period immediately following activation, the modulation of T cell activation switches from a direct regulation of AP-1 genes by FOXO1 to a FOXO1 induction of the *Bach2* transcript and the resulting competition by BACH2 for AP-1 sites.

Activation of FOXO1 or inhibition of JNK dampens CD8$^+$ T cell effector pathways

To address the phenotypic effects resulting from the absence of FOXO1 and the corresponding overexpression or overactivity of AP-1, we sought to measure T cell proliferation and the expression of effector functions. AP-1 can promote the expression of cytotoxic effector molecules, such as granzyme B (GZMB) (Hanson et al., 1993; Babichuk and Bleackley, 1997) and pro-inflammatory cytokines such as interferon γ (IFN-γ) (Cippitelli et al., 1995; Zhang et al., 1998). Since FOXO1 exerts inhibitory influences on AP-1 expression in pre-activation naive cells (Figure 1), we explored the possibility that enforced nuclear expression of FOXO1 may have an opposite effect—that is, to suppress AP-1 and hence diminish the expression of genes encoding effector molecules. Furthermore, if these effects were working as a result of AP-1 modulation, then we wished to test the prediction that the inhibition of Jun-N-terminal kinase (JNK), capable of phosphorylating JUN and ATF family members, would also enhance T cell proliferation and reduce the expression of the effector molecules GZMB and IFN-γ.

T cells from WT, *Foxo1*-KO, and *Foxo1*-AAA mice were activated in culture via anti-CD3 and anti-CD28, and cellular divisions were measured with or without a JNK inhibitor (JNKi) (Hibi et al., 1993; Barr et al., 2002) (Figures 3A and 3B). Compared with WT, T cells from *Foxo1*-KO mice displayed a diminished number of cell divisions, although T cells from *Foxo1*-AAA mice also displayed a modest but significant inhibition of recorded divisions. Consistent with a contribution of AP-1 to these phenotypic effects, a JNKi was able to enhance the number of cell divisions carried out by WT and *Foxo1*-KO T cells, and yet it did not affect the proliferation of *Foxo1*-AAA T cells that should exhibit AP-1 repression.

We assessed the expression of effector-associated GZMB in WT, *Foxo1*-KO, and *Foxo1*-AAA CD8$^+$ T cells activated *in vitro*. Compared with WT T cells, *Foxo1*-KO T cells uniformly expressed higher amounts of GZMB, whereas in *Foxo1*-AAA T cells, GZMB expression was reduced close to background levels (Figure 3C). Contrasting its enhancement of proliferation, JNKi decreased the amount of GZMB expressed in both WT and *Foxo1*-KO T cells, and again it had no consistent effect on *Foxo1*-AAA T cells, in which AP-1 is already suppressed (Figure 3D). To examine cytokine expression, we re-stimulated previously activated cultures with phorbol 12-myristate 13-acetate (PMA) plus ionomycin in the presence of a Golgi transport inhibitor, and again, *Foxo1*-KO T cells displayed an enhanced proportion of IFN-γ$^+$ T cells, along with an increased amount of IFN-γ/cell among IFN-γ$^+$ cells, compared with WT. Conversely, the proportion of IFN-γ$^+$ T cells and the amount of IFN-γ/cell was diminished in *Foxo1*-AAA T cells compared with WT (Figure 3E). In all of the cases, the effector molecule or cytokine expression was highest in *Foxo1*-KO, moderate in WT, and lowest in *Foxo1*-AAA T cells. Finally, similar to the results obtained for GZMB, both the proportion of IFN-γ$^+$ T cells and the amount of IFN-γ expressed per cell were inhibited by JNKi (Figure 3F). These results are consistent with a role for FOXO1 in the inhibition of effector function. As we showed that FOXO1 supports the suppression of AP-1 mRNA and protein, and direct suppression of AP-1 through JNK inhibition causes similar effects, we conclude that FOXO1 regulates effector versus memory differentiation, in part, through its role in attenuating AP-1 expression.

FOXO1 diminishes effector molecule expression and increases CD127^{high} cells

Previous studies showed that an acute loss of FOXO1 function just before or at the time of infection resulted in a substantial skewing of the T cell antiviral response toward an effector phenotype represented by the expression of KLRG1 and GZMB (Hess Michelini et al., 2013; Delpoux et al., 2017). We thus sought to determine how antigen-specific *Foxo1*-AAA T cells respond to a viral pathogen *in vivo* and accordingly regulate effector molecules. For this study, we performed a mixed adoptive transfer of WT P14 and *Foxo1*-AAA P14 T cells into WT hosts, infected the hosts with LCMV-ARM, and tracked the abundance and phenotype of WT P14 and *Foxo1*-AAA P14 T cells. The analysis showed a ~20-fold defect in the accumulation of *Foxo1*-AAA P14 T cells relative to WT (Figures 4A and 4B). The origin of this difference is consistent with reduced survival and the number of cells in cycle as measured by a decrease in BCL2 and Ki67 expression (Figure S3).

To determine whether *Foxo1*-AAA expression alters the differentiation decision between effector and memory precursor cells, we measured the expression of CD127 and KLRG1, in which CD127$^+$KLRG1$^-$ cells are associated with a memory precursor fate, and CD127$^-$KLRG1$^+$ cells are associated with a terminal effector fate (Kaech and Wherry, 2007). The results showed a 2-fold increase in the proportion of CD127$^+$KLRG1$^-$ *Foxo1*-AAA cells at day 7, and a more modest difference in later time points, suggesting that enforced nuclear FOXO1 expression skews responding cells toward a memory precursor fate (Figure 4C). FOXO1 has also been shown to play a role in the inhibition of TBET expression, a regulator central to effector cell programming (Kerdiles et al., 2010; Rao et al., 2012; Luo and Li, 2018), and thus, *Foxo1*-AAA would be predicted to diminish TBET expression post-activation. To avoid confounding the

(A and B) Data are cumulative from 5 experiments, with n = 2 or 3 mice per group.
(C) Data are cumulative from 4 experiments with n = 2 or 3 mice per group.
(D–F) Data are cumulative from 3 (AAA) to 4 (WT and KO) experiments, with n = 2 or 3 mice per group.
*p < 0.05; **p < 0.01; ***p < 0.001; ****p < 0.0001; unpaired (A, C, and E) or paired (B, D, and F) Student's t tests were used, and error bars represent means ± SEMs.

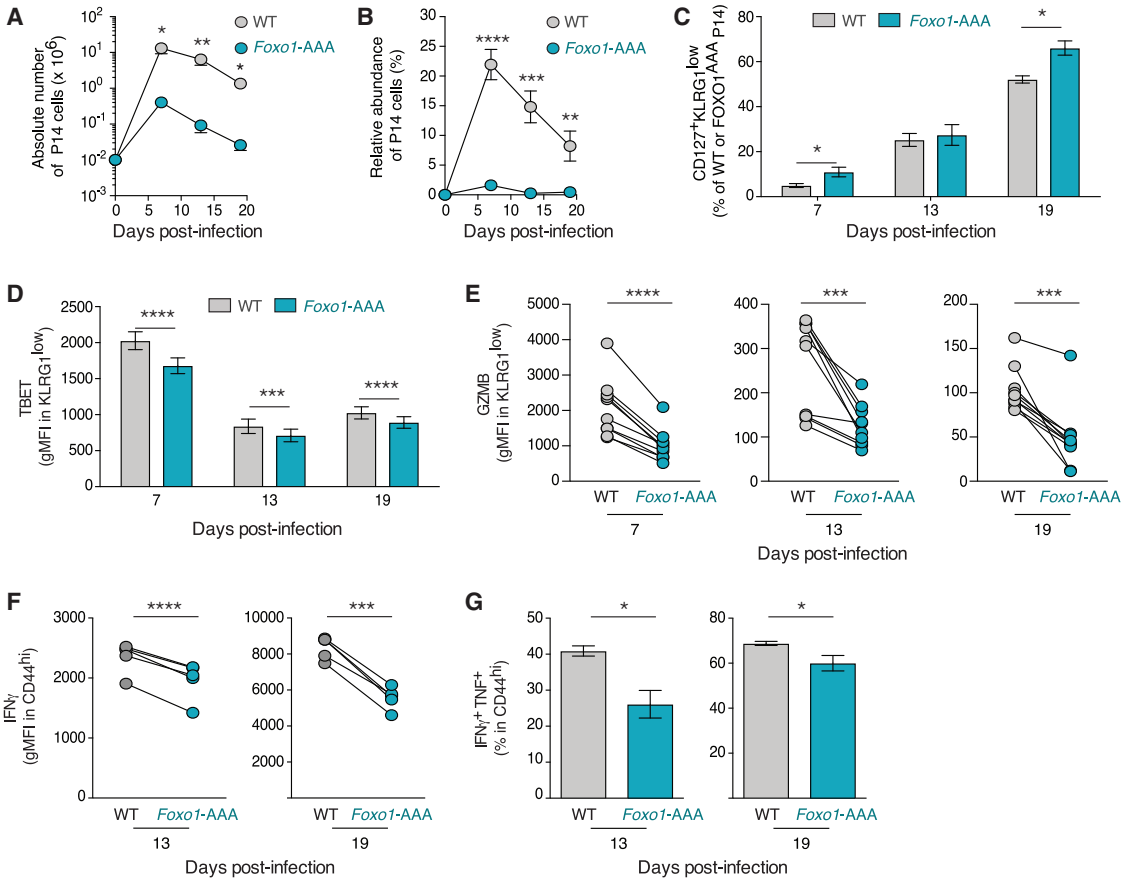

Figure 4. Nuclear expression of FOXO1 enforces stem cell-like properties characteristic of CD8⁺ T cell memory cells

(A–G) A mixed adoptive transfer of WT P14 and *Foxo1*-AAA P14 T cells into WT hosts at day −1 and infected with LCMV-ARM on day 0.

(A and B) The number (A) and relative abundance (as a percentage of the total CD8⁺ T cells) (B) of splenic WT P14 and *Foxo1*-AAA P14 cells.

(C) Differentiation as measured by CD127 and KLRG1.

(D) TBET immunostaining of KLRG1^{low} cells.

(E) GZMB immunostaining of KLRG1^{low} cells.

(F) IFN-γ gMFI in indicated cells after 4 h of PMA/IONO re-stimulation *ex vivo*.

(G) Bar graphs depict the percentage of TNF and IFN-γ double positive after stimulation with PMA/IONO for 4 h.

(A–E) Data are from 2 experiments, with 5 mice per time point.

(E and F) Data are from 1 representative experiment among 2 experiments, with 5 mice per time point.

*p < 0.05; **p < 0.01; ***p < 0.001; ****p < 0.0001; paired Student's t test was used, and error bars represent means ± SEMs.

results with the skewing of KLRG1 subsets, we gated on KLRG1^{low} P14 cells, since TBET is known to positively correlate with KLRG1 expression in WT cells. Even within the KLRG1^{low} population, we found that *Foxo1*-AAA cells expressed lower amounts of TBET than WT controls (Figure 4D). These data are consistent with decreased KLRG1^{high} differentiation in *Foxo1*-AAA cells and with the role of FOXO1 in skewing T cell differentiation toward a central memory phenotype.

Similarly, the expression of GZMB and IFN-γ effector molecules was also affected by enforced nuclear expression of FOXO1. Paired sample plotting allowed a comparison between GZMB expression from WT and *Foxo1*-AAA P14 T cells from the same host animal (Figures 4E and 4F). These data reprised our *in vitro* experiments—WT virus-specific CD8⁺ T cells expressed higher GZMB and IFN-γ than *Foxo1*-AAA virus-specific CD8⁺ T cells. This, in turn, translated into fewer polyfunctional effector cells as measured by the co-expression of IFN-γ and tumor necrosis factor (TNF) (Figure 4G). The results presented in Figures 1 through 4 are consistent with a role for FOXO1 in the inhibition of effector function. As we showed that FOXO1 supports the suppression of AP-1 mRNA and protein, and direct suppression of AP-1 through JNK inhibition causes similar effects, we conclude that FOXO1 regulates effector versus memory differentiation, in part, through its role in AP-1 expression.

Differential genomic accessibility in *Foxo1*-KO cells reflect increased effector and AP-1 signatures

We investigated transcription factor motifs found within sites of differential genomic accessibility in WT P14 and *Foxo1*-KO P14 T cells, before and after acute infection. Whereas some transcription factor motifs appeared with high frequency in these sites independent of genotype (including CTCF, CTCFL/BORIS,

ETS, and RUNX factors; data not shown), we found that WT cells showed increases in Forkhead domain binding sites, presumably associated with the opening of chromatin in the presence of FOXO1 (Figure S4A). In contrast, sites with increased genomic accessibility in *Foxo1*-KO T cells relative to WT exhibited increased binding sites for PRDM1 (BLIMP1), TBOX (TBET and EOMES), AP-1/BATF, and IRF factors—all of which are important for the development of effector function. As we have shown increased AP-1 abundance and decreased BACH2 in *Foxo1*-KO T cells relative to WT, the increased DNA accessibility in sites containing AP-1 binding sites suggest either (1) increased AP-1 autoregulation, caused by FOXO1 deletion, results in increased chromatin accessibility proximal to AP-1 genes, or (2) an undetermined aspect of FOXO1 deletion possibly reflecting its ability to recruit co-repressors.

We and others have found increased TBET mRNA and protein in *Foxo1*-KO T cells (Kerdiles et al., 2010; Rao et al., 2012; Hess Michelini et al., 2013; Kim et al., 2013), and furthermore, that the graded expression of FOXO1 can be directly correlated with TCF7 expression and inversely correlated with TBET (Delpoux et al., 2017). Therefore, an increased number of TBOX-consensus binding sites within areas of differential DNA accessibility in *Foxo1*-KO versus WT mice is consistent with the role of FOXO1 in suppressing TBET activity and inhibiting terminal effector T cell differentiation. These data are consistent with *Foxo1*-WT cells possessing increased open chromatin near memory-associated transcription factors (i.e., Forkhead and HMG-box), but relatively decreased chromatin accessibility near effector-associated molecules (i.e., TBOX) in relation to *Foxo1*-KO T cells.

The informatic analysis above renewed our interest in the FOXO1 regulation of *Bach2*. In Figure 2C we reported decreased *Bach2* mRNA in *Foxo1*-KO post-activation $CD8^+$ T cells; to further investigate this, we obtained the RNA-seq data from a study of activated T cells from *Bach2*-KO mice (Roychoudhuri et al., 2016) and plotted a fold-change-by-fold-change plot of *Foxo1*-KO versus WT and *Bach2*-KO versus WT (Figure S4B). This plot revealed that *Foxo1* and known FOXO1 target *Tcf7* (Hess Michelini et al., 2013) were minimally regulated in *Bach2*-KO versus WT T cells. However, effector molecules *Gzma* and *Gzmb* were more abundant in *Foxo1*-KO and *Bach2*-KO T cells. We then re-examined our FOXO1 ChIP-seq data (Figures 1C and 2B) and found abundant individual FOXO1 binding sites in and near the *Bach2* gene locus, with peak calling software ascribing 13 FOXO1 genomic binding sites (the 7^{th} most abundantly bound gene) in naive cells and 8 FOXO1 binding sites (the 12^{th} most abundantly bound gene) in day 12 p.i. $CD8^+$ P14 cells (Figures S4C and S4D). The binding sites nearest the gene locus are depicted in Figure 2B. The above analysis is consistent with FOXO1 directly binding to the gene locus and nearby enhancers and positively regulating *Bach2* mRNA/protein abundance. This, in turn, regulates effector molecules such as GZMB, likely through the binding of AP-1 sites as previously reported (Roychoudhuri et al., 2016).

Loss of FOXO1 expression leads to chronic activation in T cells surviving virus infection

As previously presented, WT T cells and T cells acutely deleted for *Foxo1* initially expand with the same kinetics in response to infection with LCMV-ARM (Figure 5A). However, at 30 days p.i., the number of *Foxo1*-KO T cells was diminished compared to WT. This is in part due to the observation that by day 30 p.i., there are few, if any, *Foxo1*-KO memory T cells with the ability to undergo reactivation and proliferation in response to an antigenic re-challenge (Hess Michelini et al., 2013). The population of *Foxo1*-KO T cells 30 days p.i. displayed higher amounts of FOS, JUNB, and FOSB (Figure 5B). This presented the possibility that FOXO1-deficient cells are unable to completely regain quiescence and may exhibit signs of chronic activation that could lead to a state of exhaustion or senescence, as described for chronically activated T cells in human beings (Plunkett et al., 2005; Chapman and Chi, 2018).

To assess this issue, we sought to examine the physiology of long-lived T cells subsequent to virus infection, especially that associated with chronic activation: increased frequency of apoptosis, evidence of activation, loss of co-receptor expression, an inability to produce multiple effector cytokines, or the induction of multiple inhibitory receptors (Effros, 1997; Parish et al., 2010). Apoptosis was examined by the presence of a cleaved and activated form of CASP3 (ActCASP3). Within $CD44^-$ naive T cells, there was a significant increase in the steady-state number of $ActCASP3^+$ cells with the loss of *Foxo1*, and such an increase was even more substantial in the day 30 population of T cells with a memory-like $KLRG1^{low}$ phenotype (Figure 5C). Strikingly, a similar result was found for the expression of CD69 as an indication of cellular activation. Whereas there was an ~3-fold increase in the number of $CD69^+$ *Foxo1*-KO naive T cells compared to WT, the proportion of *Foxo1*-KO, $KLRG1^-$ memory-like T cells that continued to express CD69 was increased by ~15-fold over that of WT (Figure 5D).

Further analysis of day 30 T cells showed that within the population of $KLRG1^-$ T cells, few were $Ki67^+$, and yet there was a large population that sustained the expression of GZMB (Figures S5A and S5B). As suggested by Figure 1A, the proportion of naive T cells capable of IFN-γ production was increased in the absence of *Foxo1* (Figure S5C).

One hallmark of exhaustion as defined for T cells from mice or human beings infected with a persistent virus is the expression of the inhibitory receptors (Wherry et al., 2007; Wherry and Kurachi, 2015). Despite the high expression of CD69 and AP-1 at day 30 p.i., there was a virtually undetectable number of *Foxo1*-KO T cells that expressed in PD-1, LAG-3, or TIM3 (Figure S5D). This would seem to separate the concept of "exhaustion" associated with receptor-based inhibitory signaling from the form of chronic activation exhibited by *Foxo1*-KO T cells. Rather, T cells that lack *Foxo1* appear to have characteristics of end-stage effector cells. They include a greater proportion of cells expressing CX3CR1 (fractalkine receptor) (Böttcher et al., 2015) (Figure S5E) and a reduced proportion expressing CD27, the loss of which is characteristic of fully differentiated effector T cells (Grant et al., 2017) (Figure S5F).

A concept that is associated with chronic infections, cancer, or autoimmunity in human beings is T cell replicative senescence. It is most consistently characterized by the loss of CD28 in both CD4 and CD8 T cells, but in addition, it can include defects in replication, shortened telomeres, and elevated production of

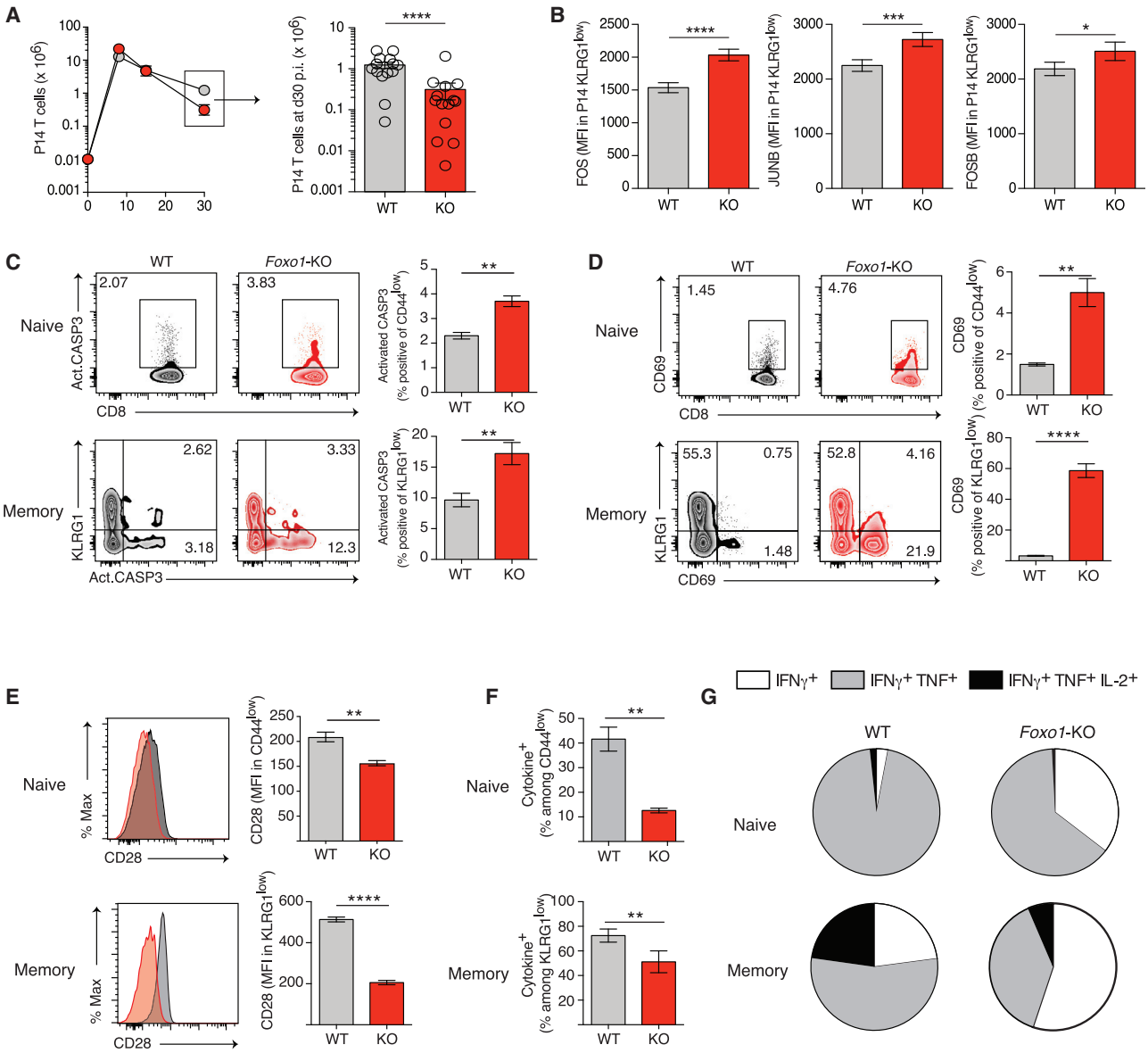

Figure 5. Naive and memory *Foxo1*-KO CD8 T cells exhibit a senescent phenotype

(A–F) Adoptive transfer of WT P14 and *Foxo1*-KO P14 T cells into WT hosts at day −1 and infected with LCMV-ARM on day 0.

(A) Absolute number of WT P14 and *Foxo1*-KO P14 cells over time (left) and at day 30 p.i. (right).

(B) AP-1 factor immunostaining was determined at day 30 p.i. for KLRG1^{low} WT and *Foxo1*-KO P14 cells.

(C) Expression of KLRG1 and Act-caspase-3 by WT and *Foxo1*-KO P14 cells before and 30 days p.i.

(D) Expression of KLRG1 and CD69 by WT and *Foxo1*-KO P14 cells before and 30 days p.i.

(E) Expression of CD28 by WT and *Foxo1*-KO P14 cells 30 days p.i.

(F) The proportion of P14 T cells expressing either TNF, IFN-γ, or both upon stim.

(G) Proportion of T cells expressing the indicated cytokines upon stim. Upper panel indicates the polyfunctionality among KLRG1^{low} cells (day 30); lower panel, indicates naive T cells.

(A) Data are cumulative from 2 to 4 experiments, with minimum n = 3 mice per group and per time point. (B) Data are cumulative from 2 experiments, with n = 5 mice per group. (C–G) Data are cumulative from 2 experiments, with minimum n = 3 mice per group and per experiment.

*p < 0.05; **p < 0.01; ***p < 0.001; ****p < 0.0001; paired (A–G) and unpaired (C–G) Student's t tests were used, and error bars represent means ± SEMs.

inflammatory cytokines (Vallejo, 2005; Henson et al., 2012; Chou and Effros, 2013). In *Foxo1*-KO T cells, CD28 was uniformly reduced in naive T cells, and it was even more reduced in P14 *Foxo1*-KO KLRG1^{low} day 30 post-infection T cells, compared with WT (Figure 5E). A further indication of senescence is the inability of T cells to produce effector cytokines upon stimulation: TNF, IFN-γ, and interleukin-2 (IL-2). This was measured as the proportion of cytokine-expressing T cells (positive for TNF,

IFN-γ, or both), and was found to be diminished in T cells from *Foxo1*-KO mice compared with WT (Figure 5F). Furthermore, the ability to simultaneously produce multiple cytokines, especially TNF, IFN-γ, and IL-2, is a property of functional memory T cells, and as depicted in Figure 5G, *Foxo1*-KO mice possessed proportionately fewer double- and triple-cytokine-producing T cells. These data indicate that FOXO1 is required to stave off the onset of a phenotypic unresponsiveness in T cells that is similar to that found in elderly human beings, especially in those T cells specific for chronic viruses such as human cytomegalovirus (Henson et al., 2012; Chou and Effros, 2013).

Expression of FOXO1 inversely correlates with a senescent phenotype acquired with age

To determine whether the effects of aging T cells are manifest in the expression of FOXO1, we sought to analyze T cells derived from human subjects of different ages. Human $CD8^+$ T cells can be classified through the expression of CD45RA and CD27 (Hamann et al., 1997; Kern et al., 1999; Sallusto et al., 1999)—naive, T_N: $CD45RA^+$ $CD27^+$; central memory T_{CM}: $CD45RA^-$ $CD27^+$; effector memory, T_{EM}: $CD45RA^-$ $CD27^-$; and effector memory that have re-expressed CD45RA, T_{EMRA}: $CD45RA^{int}$ $CD27^-$. Most of the T_{EMRA} cells also express CD57 and KLRG1, and these are indicators of senescence (Brenchley et al., 2003) (Figure 6A). Each of the described $CD8^+$ T cell subsets was characterized for FOXO1 expression, and as shown, there was a clear hierarchy. T_N expressed the most FOXO1, followed by T_{CM}, T_{EM}, and senescent T_{EMRA} cells (Figure 6B).

TCF7 is a transcription factor that is essential for the formation of memory T cells, and its expression is part of a program of gene expression that is predictive of $CD8^+$ T cells that will respond to chronic viral infections (Utzschneider et al., 2016; Wu et al., 2016; Lin et al., 2016) or tumors following checkpoint therapy (Zhou et al., 2010; Jeannet et al., 2010; Sade-Feldman et al., 2018; McLane et al., 2019; Siddiqui et al., 2019). Importantly, it is wholly dependent on FOXO1 for expression in mouse $CD8^+$ T cells post-activation (Hess Michelini et al., 2013), and as such, it showed the very same hierarchy of expression $T_N > T_{CM} > T_{EM} > T_{EMRA}$ (Figure 6C). A further comparison was carried out to examine the possibility that with diminished FOXO1 and TCF7 expression, AP-1 expression would be increased. The results showed that FOS and FOSB were clearly expressed in higher amounts in senescent compared to naive T cells, although this did not appear to be true for JUNB (Figure 6D).

To explore a connection between T cell senescence and aging, a comparison was made between blood from neonates (umbilical cord), healthy young adults, and elderly volunteers. In the representative example shown, $CD8^+$ T cells from neonates were entirely contained within T_N and T_{CM} subsets, young adults acquired T_{EM} and T_{EMRA} subsets, and the elderly possessed predominantly T_{EMRA} cells (Figure 6E). Looking at the amount of FOXO1 expression $CD8^+$ T_N cells, there was a strong and linear negative correlation between FOXO1 abundance and age (Figure 6F), and again, the very same correlation was found for TCF7 (Figure 6G). The inverse of these correlations was seen for FOS and FOSB but, again, not JUNB. Looking at young versus elderly donor T_N cells, there was a significant increase in the FOS family factors (Figure 6H).

Laboratory mice are considered "old" for aging studies between 18 and 24 months (the equivalent in human beings is 56–69 years) (Flurkey et al., 2007; Weon and Je, 2012); however, specific pathogen-free (SPF) aged mice cannot be considered an accurate model for aged, disease-experienced, vaccinated human beings. Nonetheless, we wanted to examine whether T cells from aged SPF mice would recapitulate some of the hallmarks of aged, senescent cells that were observed in human beings. We observed a decrease in FOXO1 geometric mean fluorescence intensity (gMFI) in naive T cells from old mice versus young mice (Figure S6A), although the changes in the amounts of AP-1 in naive T cells were only marginally affected (Figure S6B). However, there was a substantial and significant decrease in $CD62L^{hi}$ ($CD8^+CD44^-$) T cells along with an increase in CD69 expression and a decrease in CD28 expression (Figures S6C–S6E), all correlates of T cell senescence. Similarly, the number of naive $CD8^+$ T cells in cycle was reduced (Figure S6F). These data recapitulate the key findings from the human studies—that naive ($CD44^{low}$) T cells from older mice express less FOXO1 and more of 2 of the 3 AP-1 factors tested.

In summary, there is an age-dependent loss of FOXO1 and TCF7 expression and an increase in FOS expression that correlates in human $CD8^+$ T cells with the appearance of T_{EMRA} cells at the expense of T_N and T_{CM} cells. Along with our analysis of a loss-of-function and constitutively active mutations in mice, these data reveal a role for FOXO1 in suppressing T cell activation, in part, by attenuation of AP-1 factors, allowing the maintenance of naive and memory T cells in a state of antigen responsiveness.

DISCUSSION

T cells are integral to organismal homeostasis. If they are diminished in function or number, then commensal and infectious microbial and viral agents are overly virulent (as in AIDS), and yet, T cells are intrinsically capable of injuring their host. As such, the induction of T cell effector function is balanced on a knife edge and regulated by strong and elaborate negative feedback control. FOXO transcription factors have been found to be essential to many aspects of adaptive immunity (Ouyang and Li, 2011; Hedrick et al., 2012), and in particular, they allow antigen-activated and expanded $CD8^+$ T cells to maintain stem cell-like qualities of self-renewal (Rao et al., 2012; Hess Michelini et al., 2013; Kim et al., 2013). In this report, we show that FOXO1 is continually required to prevent or suppress a state of activation in naive and post-activation $CD8^+$ T cells, respectively, and in so doing, prevent the onset of senescence in the $CD8^+$ T cell population. The mechanism is, in part, the active suppression of the AP-1 transcription factors, factors known to be central to many signaling pathways important for immune system activation (Foletta et al., 1998; Wisdom, 1999; Shaulian and Karin, 2002).

These genetic data observed in mice have a correlate with the natural progression of T cell differentiation. Human T cells lose stem cell qualities with antigen-mediated activation as they progress from naive T cells ($CD27^+CD45RA^{high}$) and central memory ($CD27^+CD45RA^-$) T cells to effector memory ($CD27^-CD45RA^-$) T cells and finally acquire a T_{EMRA} phenotype that exhibits intermediate expression of CD45RA, a lack of

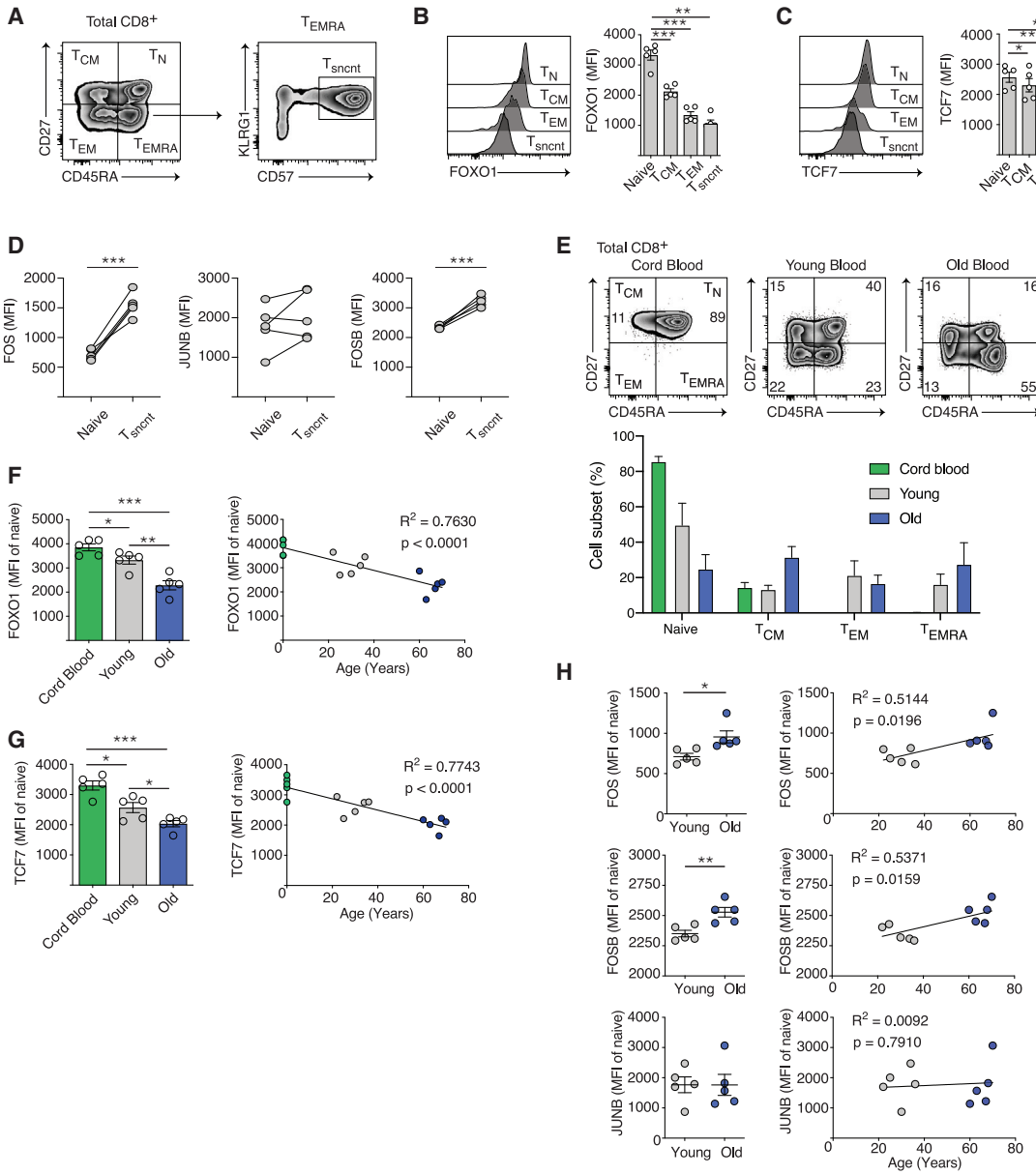

Figure 6. Age-dependent, inverse correlation of FOXO1 and AP-1 subunit abundance in human T cells

(A) Total CD8$^+$ T cells analyzed for CD27 and CD45RA (left). Senescent T cells (T_{sncnt}) were analyzed by KLRG1 versus CD57 expression (right). Representative data from young adult cohort are shown.

(B) FOXO1 abundance among different CD8$^+$ T cell subsets (as identified by gating in A); the bar graph at right depicts FOXO1 expression across the indicated number (dots) of biological replicates.

(C) TCF7 abundance among different CD8$^+$ T cell subsets; the bar graph at right depicts TCF7 expression across the indicated number (dots) of biological samples.

(D) FOS, JUNB, and FOSB abundance determined among naive and senescent CD8$^+$ T cells. Data were derived from individual young adult patient samples.

(E) Expression of CD27 and CD45RA from a representative sample of each age group: cord blood, young adult, and elderly.

(F) Quantitation of FOXO1 among naive CD8$^+$ T cells in cord blood, young adult, and elderly adult blood samples. The curve depicts a linear regression of FOXO1 expression versus the age of the patients for CD8$^+$ T cells.

(G) Quantitation of TCF7 among naive CD8$^+$ T cells in cord blood, young adult, and elderly adult blood samples. The curve depicts a linear regression of TCF7 expression versus the age of the patients for CD8$^+$ T cells.

(H) Quantitation of FOS, JUNB, and FOSB (MFI) among naive CD8$^+$ T cells from young and elderly adult blood samples. The curves represent the linear regression AP-1 expression versus the age of the patients among naive CD8$^+$ T cells.

(A–H) Data represent 5 independent samples per group.

*p < 0.05; **p < 0.01; ***p < 0.001; ****p < 0.0001; paired Student's t test was used (B–D), unpaired Student's t test was used (F–H), and error bars represent means ± SEMs.

CD27, and strong expression of CD57 and KLRG1 (Goronzy and Weyand, 2019). The data presented here indicate that the stepwise loss of "stemness" is inversely correlated with FOXO1 in the control of TCF7 expression. Moreover, in comparing naive to T_{EMRA} cells, an increase in the expression of two AP-1 subunits, FOS and FOSB, was observed, although curiously, not JUNB.

The progression $T_N \rightarrow T_{CM} \rightarrow T_{EM} \rightarrow T_{EMRA}$ also correlates with aging, as cord blood almost entirely consisted of naive T cells, young adult blood contained approximately equivalent proportions of all four subsets, and blood from old subjects was largely made up of T_{EMRA} cells. Even cells meeting the commonly used definition of naive human T cells, $CD45RA^+CD27^+$, displayed a decrease in FOXO1 and TCF7 with age of the donor. We conclude that the appearance of a senescent phenotype correlates with reduced FOXO1 and corresponding changes in TCF7 and certain AP-1 subunits. We propose that, given the close association between the phenotypes we recorded in mouse and human cells, the senescence phenotype in T cells is mechanistically dependent on the amount of FOXO1 expression. Although FOXO1 is negatively regulated by growth factors that cause phosphorylation and nuclear localization, other types of transcriptional or post-translation regulatory mechanisms may also contribute to its lack of abundance in aging T cells. Of interest is whether nutrient abundance or the resulting manifestations of obesity, stress, and chronic inflammation can affect the amount of FOXO1 and thus the progression of immune senescence.

Aging is slowed in nematodes and flies when insulin-like signaling is reduced, similar to the effects of calorie restriction, and this enhanced longevity originates from a lack of inhibitory FOXO phosphorylation and the resulting FOXO-regulated gene transcription (Burgering, 2008; Salih and Brunet, 2008). Remarkably, there are indications that a similar process is found in human beings; genome-wide association studies have revealed FOXO1 and FOXO3 to be the most prominent among a small number of genes associated with increased age at death or age at natural menopause (Lunetta et al., 2007; Li et al., 2009; Kenyon, 2010; Anselmi et al., 2009; Flachsbart et al., 2009; Willcox et al., 2008). Since FOXO transcription factors are prominently involved in the insulin signaling pathway and are known to control glucose metabolism in most, if not all organs, one idea is that similar to nematodes and flies, the key to FOXO regulation of longevity resides in its control of energy utilization (Kousteni, 2012). However, FOXO transcription factors play roles in many other aspects of physiology, including stress resistance, cell-cycle progression, apoptosis, and immunity (Hedrick et al., 2012; Martins et al., 2016). In addition, FOXO1 is important in the regulation of genes involved in maintaining the pluripotency and characteristics of stem cells (Zhang et al., 2011). This is a pathway that most likely originated early in metazoan evolution as FOXO was found to be key to the self-renewal of all three stem cell lineages in Hydra, an immortal cnidarian genus diverged from bilateral phyla on the order of 600 million years ago (Boehm et al., 2012).

If immune plasticity is a factor in the aging process (Xu and Larbi, 2017; Goronzy and Weyand, 2017), then these data imply that one of the many ways in which FOXO transcription factors may affect longevity could include the maintenance of an effective adaptive immune system. With a diminished number of T cells capable of serial reactivation and renewal, and thus a reduced antigen-reactive repertoire, the inflammation and stress induced by infectious agents or cancer may accelerate aging averaged over an entire population.

STAR★METHODS

Detailed methods are provided in the online version of this paper and include the following:

- KEY RESOURCES TABLE
- RESOURCE AVAILABILITY
  - Lead contact
  - Materials availability
  - Data and code availability
- EXPERIMENTAL MODEL AND SUBJECT DETAILS
  - Mice and tamoxifen treatment
  - Adoptive transfers and infection
- METHOD DETAILS
  - Immunofluorescent staining and flow cytometry
  - Immunoblotting for FOXO1 and pFOXO-S253
  - Cytokine detection
  - *In vitro* assays
  - ChIP-seq, RNA-seq, and ATAC-seq
  - Human samples and immunostaining
- QUANTIFICATION AND STATISTICAL ANALYSIS

SUPPLEMENTAL INFORMATION

Supplemental Information can be found online at https://doi.org/10.1016/j.celrep.2020.108674.

ACKNOWLEDGMENTS

This work was supported by the National Institutes of Health (U.S.A.) grants R01AI073885 and R01AI103440 to S.M.H. We thank Ming Li (Memorial Sloan Kettering) for providing the *Foxo1*-AAA mice. Allen Yaldiko carried out genotyping, assisted in the maintenance of animal colonies, and contributed to essential biochemical experiments. This work is published in memory of A.D., who passed away during the preparation of this manuscript.

AUTHOR CONTRIBUTIONS

A.D., R.H.M., S.M.H. and A.L.D. conceived the study and analyzed the data. A.D. and N.M. performed the experiments and analyzed the data. S.M.Q.-P. and C.M. obtained and analyzed the human samples. S.M.H. and A.L.D. wrote the manuscript. C.D.K. and R.H.M. performed the ChIP-seq and ATAC-seq experiments. K.A.A. performed the RNA-seq experiments. K.K. and L.L. established the human cohort/provided blood samples. A.L.D. analyzed the RNA-seq data, and A.L.D. and C.D.K. analyzed the ATAC-seq and ChIP-seq data. All of the authors reviewed the manuscript.

DECLARATION OF INTERESTS

The authors declare no competing interests.

Received: October 16, 2019
Revised: October 25, 2020
Accepted: December 29, 2020
Published: January 26, 2019

REFERENCES

Angel, P., Hattori, K., Smeal, T., and Karin, M. (1988). The jun proto-oncogene is positively autoregulated by its product, Jun/AP-1. Cell *55*, 875–885.

Anselmi, C.V., Malovini, A., Roncarati, R., Novelli, V., Villa, F., Condorelli, G., Bellazzi, R., and Puca, A.A. (2009). Association of the FOXO3A locus with extreme longevity in a southern Italian centenarian study. Rejuvenation Res. *12*, 95–104.

Babichuk, C.K., and Bleackley, R.C. (1997). Mutational analysis of the murine granzyme B gene promoter in primary T cells and a T cell clone. J. Biol. Chem. *272*, 18564–18571.

Barr, R.K., Kendrick, T.S., and Bogoyevitch, M.A. (2002). Identification of the critical features of a small peptide inhibitor of JNK activity. J. Biol. Chem. *277*, 10987–10997.

Blankenberg, D., Gordon, A., Von Kuster, G., Coraor, N., Taylor, J., and Nekrutenko, A.; Galaxy Team (2010). Manipulation of FASTQ data with Galaxy. Bioinformatics *26*, 1783–1785.

Boehm, A.M., Khalturin, K., Anton-Erxleben, F., Hemmrich, G., Klostermeier, U.C., Lopez-Quintero, J.A., Oberg, H.H., Puchert, M., Rosenstiel, P., Wittlieb, J., and Bosch, T.C. (2012). FoxO is a critical regulator of stem cell maintenance in immortal Hydra. Proc. Natl. Acad. Sci. USA *109*, 19697–19702.

Böttcher, J.P., Beyer, M., Meissner, F., Abdullah, Z., Sander, J., Höchst, B., Eickhoff, S., Rieckmann, J.C., Russo, C., Bauer, T., et al. (2015). Functional classification of memory CD8(+) T cells by CX3CR1 expression. Nat. Commun. *6*, 8306.

Brenchley, J.M., Karandikar, N.J., Betts, M.R., Ambrozak, D.R., Hill, B.J., Crotty, L.E., Casazza, J.P., Kuruppu, J., Migueles, S.A., Connors, M., et al. (2003). Expression of CD57 defines replicative senescence and antigen-induced apoptotic death of CD8+ T cells. Blood *101*, 2711–2720.

Brunet, A., Park, J., Tran, H., Hu, L.S., Hemmings, B.A., and Greenberg, M.E. (2001). Protein kinase SGK mediates survival signals by phosphorylating the forkhead transcription factor FKHRL1 (FOXO3a). Mol. Cell. Biol. *21*, 952–965.

Buenrostro, J.D., Giresi, P.G., Zaba, L.C., Chang, H.Y., and Greenleaf, W.J. (2013). Transposition of native chromatin for fast and sensitive epigenomic profiling of open chromatin, DNA-binding proteins and nucleosome position. Nat. Methods *10*, 1213–1218.

Burgering, B.M. (2008). A brief introduction to FOXOlogy. Oncogene *27*, 2258–2262.

Burgering, B.M., and Kops, G.J. (2002). Cell cycle and death control: long live Forkheads. Trends Biochem. Sci. *27*, 352–360.

Calnan, D.R., and Brunet, A. (2008). The FoxO code. Oncogene *27*, 2276–2288.

Chapman, N.M., and Chi, H. (2018). Hallmarks of T-cell exit from quiescence. Cancer Immunol. Res. *6*, 502–508.

Chou, J.P., and Effros, R.B. (2013). T cell replicative senescence in human aging. Curr. Pharm. Des. *19*, 1680–1698.

Cippitelli, M., Sica, A., Viggiano, V., Ye, J., Ghosh, P., Birrer, M.J., and Young, H.A. (1995). Negative transcriptional regulation of the interferon-gamma promoter by glucocorticoids and dominant negative mutants of c-Jun. J. Biol. Chem. *270*, 12548–12556.

Delpoux, A., Poitrasson-Rivière, M., Le Campion, A., Pommier, A., Yakonowsky, P., Jacques, S., Letourneur, F., Randriamampita, C., Lucas, B., and Auffray, C. (2012). Foxp3-independent loss of regulatory CD4+ T-cell suppressive capacities induced by self-deprivation. Eur. J. Immunol. *42*, 1237–1249.

Delpoux, A., Lai, C.Y., Hedrick, S.M., and Doedens, A.L. (2017). FOXO1 opposition of $CD8^+$ T cell effector programming confers early memory properties and phenotypic diversity. Proc. Natl. Acad. Sci. USA *114*, E8865–E8874.

Delpoux, A., Michelini, R.H., Verma, S., Lai, C.Y., Omilusik, K.D., Utzschneider, D.T., Redwood, A.J., Goldrath, A.W., Benedict, C.A., and Hedrick, S.M. (2018). Continuous activity of Foxo1 is required to prevent anergy and maintain the memory state of $CD8^+$ T cells. J. Exp. Med. *215*, 575–594.

Dutko, F.J., and Oldstone, M.B. (1983). Genomic and biological variation among commonly used lymphocytic choriomeningitis virus strains. J. Gen. Virol. *64*, 1689–1698.

Effros, R.B. (1997). Loss of CD28 expression on T lymphocytes: a marker of replicative senescence. Dev. Comp. Immunol. *21*, 471–478.

Flachsbart, F., Caliebe, A., Kleindorp, R., Blanché, H., von Eller-Eberstein, H., Nikolaus, S., Schreiber, S., and Nebel, A. (2009). Association of FOXO3A variation with human longevity confirmed in German centenarians. Proc. Natl. Acad. Sci. USA *106*, 2700–2705.

Flurkey, K., Currer, J.M., and Harrison, D.E. (2007). The Mouse in Aging Research. In The Mouse in Biomedical Research, Second Edition, J.G.E.A. Fox, ed. (Elsevier), pp. 637–672.

Foletta, V.C., Segal, D.H., and Cohen, D.R. (1998). Transcriptional regulation in the immune system: all roads lead to AP-1. J. Leukoc. Biol. *63*, 139–152.

Gazon, H., Barbeau, B., Mesnard, J.M., and Peloponese, J.M., Jr. (2018). Hijacking of the AP-1 Signaling Pathway during Development of ATL. Front. Microbiol. *8*, 2686.

Giardine, B., Riemer, C., Hardison, R.C., Burhans, R., Elnitski, L., Shah, P., Zhang, Y., Blankenberg, D., Albert, I., Taylor, J., et al. (2005). Galaxy: a platform for interactive large-scale genome analysis. Genome Res. *15*, 1451–1455.

Goecks, J., Nekrutenko, A., and Taylor, J.; Galaxy Team (2010). Galaxy: a comprehensive approach for supporting accessible, reproducible, and transparent computational research in the life sciences. Genome Biol. *11*, R86.

Goronzy, J.J., and Weyand, C.M. (2017). Successful and Maladaptive T Cell Aging. Immunity *46*, 364–378.

Goronzy, J.J., and Weyand, C.M. (2019). Mechanisms underlying T cell ageing. Nat. Rev. Immunol. *19*, 573–583.

Gottlieb, S., and Ruvkun, G. (1994). daf-2, daf-16 and daf-23: genetically interacting genes controlling Dauer formation in Caenorhabditis elegans. Genetics *137*, 107–120.

Grant, E.J., Nüssing, S., Sant, S., Clemens, E.B., and Kedzierska, K. (2017). The role of CD27 in anti-viral T-cell immunity. Curr. Opin. Virol. *22*, 77–88.

Guertin, D.A., Stevens, D.M., Thoreen, C.C., Burds, A.A., Kalaany, N.Y., Moffat, J., Brown, M., Fitzgerald, K.J., and Sabatini, D.M. (2006). Ablation in mice of the mTORC components raptor, rictor, or mLST8 reveals that mTORC2 is required for signaling to Akt-FOXO and PKCalpha, but not S6K1. Dev. Cell *11*, 859–871.

Gustafson, C.E., Cavanagh, M.M., Jin, J., Weyand, C.M., and Goronzy, J.J. (2018). Functional pathways regulated by microRNA networks in CD8 T-cell aging. Aging Cell *18*, 12879.

Hamann, D., Baars, P.A., Rep, M.H., Hooibrink, B., Kerkhof-Garde, S.R., Klein, M.R., and van Lier, R.A. (1997). Phenotypic and functional separation of memory and effector human CD8+ T cells. J. Exp. Med. *186*, 1407–1418.

Hanson, R.D., Grisolano, J.L., and Ley, T.J. (1993). Consensus AP-1 and CRE motifs upstream from the human cytotoxic serine protease B (CSP-B/CGL-1) gene synergize to activate transcription. Blood *82*, 2749–2757.

Hedrick, S.M., Hess Michelini, R., Doedens, A.L., Goldrath, A.W., and Stone, E.L. (2012). FOXO transcription factors throughout T cell biology. Nat. Rev. Immunol. *12*, 649–661.

Heinz, S., Benner, C., Spann, N., Bertolino, E., Lin, Y.C., Laslo, P., Cheng, J.X., Murre, C., Singh, H., and Glass, C.K. (2010). Simple combinations of lineage-determining transcription factors prime cis-regulatory elements required for macrophage and B cell identities. Mol. Cell *38*, 576–589.

Henson, S.M., Riddell, N.E., and Akbar, A.N. (2012). Properties of end-stage human T cells defined by CD45RA re-expression. Curr. Opin. Immunol. *24*, 476–481.

Hess Michelini, R., Doedens, A.L., Goldrath, A.W., and Hedrick, S.M. (2013). Differentiation of CD8 memory T cells depends on Foxo1. J. Exp. Med. *210*, 1189–1200.

Hibi, M., Lin, A., Smeal, T., Minden, A., and Karin, M. (1993). Identification of an oncoprotein- and UV-responsive protein kinase that binds and potentiates the c-Jun activation domain. Genes Dev. *7*, 2135–2148.

Im, S.H., and Rao, A. (2004). Activation and deactivation of gene expression by Ca2+/calcineurin-NFAT-mediated signaling. Mol. Cells *18*, 1–9.

Jeannet, G., Boudousquié, C., Gardiol, N., Kang, J., Huelsken, J., and Held, W. (2010). Essential role of the Wnt pathway effector Tcf-1 for the establishment of functional CD8 T cell memory. Proc. Natl. Acad. Sci. USA *107*, 9777–9782.

Kaech, S.M., and Wherry, E.J. (2007). Heterogeneity and cell-fate decisions in effector and memory CD8+ T cell differentiation during viral infection. Immunity *27*, 393–405.

Kent, W.J., Sugnet, C.W., Furey, T.S., Roskin, K.M., Pringle, T.H., Zahler, A.M., and Haussler, D. (2002). The human genome browser at UCSC. Genome Res. *12*, 996–1006.

Kenyon, C.J. (2010). The genetics of ageing. Nature *464*, 504–512.

Kenyon, C., Chang, J., Gensch, E., Rudner, A., and Tabtiang, R. (1993). A C. elegans mutant that lives twice as long as wild type. Nature *366*, 461–464.

Kerdiles, Y.M., Beisner, D.R., Tinoco, R., Dejean, A.S., Castrillon, D.H., DePinho, R.A., and Hedrick, S.M. (2009). Foxo1 links homing and survival of naive T cells by regulating L-selectin, CCR7 and interleukin 7 receptor. Nat. Immunol. *10*, 176–184.

Kerdiles, Y.M., Stone, E.L., Beisner, D.R., McGargill, M.A., Ch'en, I.L., Stockmann, C., Katayama, C.D., and Hedrick, S.M. (2010). Foxo transcription factors control regulatory T cell development and function. Immunity *33*, 890–904.

Kern, F., Khatamzas, E., Surel, I., Frömmel, C., Reinke, P., Waldrop, S.L., Picker, L.J., and Volk, H.D. (1999). Distribution of human CMV-specific memory T cells among the CD8pos. subsets defined by CD57, CD27, and CD45 isoforms. Eur. J. Immunol. *29*, 2908–2915.

Kim, M.V., Ouyang, W., Liao, W., Zhang, M.Q., and Li, M.O. (2013). The transcription factor Foxo1 controls central-memory CD8+ T cell responses to infection. Immunity *39*, 286–297.

Kim, D., Langmead, B., and Salzberg, S.L. (2015). HISAT: a fast spliced aligner with low memory requirements. Nat. Methods *12*, 357–360.

Kousteni, S. (2012). FoxO1, the transcriptional chief of staff of energy metabolism. Bone *50*, 437–443.

Langmead, B., and Salzberg, S.L. (2012). Fast gapped-read alignment with Bowtie 2. Nat. Methods *9*, 357–359.

Li, Y., Wang, W.J., Cao, H., Lu, J., Wu, C., Hu, F.Y., Guo, J., Zhao, L., Yang, F., Zhang, Y.X., et al. (2009). Genetic association of FOXO1A and FOXO3A with longevity trait in Han Chinese populations. Hum. Mol. Genet. *18*, 4897–4904.

Li, P., Spolski, R., Liao, W., Wang, L., Murphy, T.L., Murphy, K.M., and Leonard, W.J. (2012). BATF-JUN is critical for IRF4-mediated transcription in T cells. Nature *490*, 543–546.

Liang, R., and Ghaffari, S. (2018). Stem Cells Seen Through the FOXO Lens: An Evolving Paradigm. Curr. Top. Dev. Biol. *127*, 23–47.

Lin, Y.C., Jhunjhunwala, S., Benner, C., Heinz, S., Welinder, E., Mansson, R., Sigvardsson, M., Hagman, J., Espinoza, C.A., Dutkowski, J., et al. (2010). A global network of transcription factors, involving E2A, EBF1 and Foxo1, that orchestrates B cell fate. Nat Immunol *11*, 635–643.

Lin, W.W., Nish, S.A., Yen, B., Chen, Y.H., Adams, W.C., Kratchmarov, R., Rothman, N.J., Bhandoola, A., Xue, H.H., and Reiner, S.L. (2016). $CD8^+$ T Lymphocyte Self-Renewal during Effector Cell Determination. Cell Rep. *17*, 1773–1782.

Lunetta, K.L., D'Agostino, R.B.S., Sr., Karasik, D., Benjamin, E.J., Guo, C.Y., Govindaraju, R., Kiel, D.P., Kelly-Hayes, M., Massaro, J.M., Pencina, M.J., et al. (2007). Genetic correlates of longevity and selected age-related phenotypes: a genome-wide association study in the Framingham Study. BMC Med. Genet. *8* (*Suppl 1*), S13.

Luo, C.T., and Li, M.O. (2018). Foxo transcription factors in T cell biology and tumor immunity. Semin. Cancer Biol. *50*, 13–20.

Martins, R., Lithgow, G.J., and Link, W. (2016). Long live FOXO: unraveling the role of FOXO proteins in aging and longevity. Aging Cell *15*, 196–207.

McLane, L.M., Abdel-Hakeem, M.S., and Wherry, E.J. (2019). CD8 T Cell Exhaustion During Chronic Viral Infection and Cancer. Annu. Rev. Immunol. *37*, 457–495.

McLaughlin, C.N., and Broihier, H.T. (2018). Keeping Neurons Young and Foxy: FoxOs Promote Neuronal Plasticity. Trends Genet. *34*, 65–78.

Ouyang, W., and Li, M.O. (2011). Foxo: in command of T lymphocyte homeostasis and tolerance. Trends Immunol. *32*, 26–33.

Ouyang, W., Liao, W., Luo, C.T., Yin, N., Huse, M., Kim, M.V., Peng, M., Chan, P., Ma, Q., Mo, Y., et al. (2012). Novel Foxo1-dependent transcriptional programs control T(reg) cell function. Nature *491*, 554–559.

Paik, J.H., Kollipara, R., Chu, G., Ji, H., Xiao, Y., Ding, Z., Miao, L., Tothova, Z., Horner, J.W., Carrasco, D.R., et al. (2007). FoxOs are lineage-restricted redundant tumor suppressors and regulate endothelial cell homeostasis. Cell *128*, 309–323.

Parish, S.T., Wu, J.E., and Effros, R.B. (2010). Sustained CD28 expression delays multiple features of replicative senescence in human CD8 T lymphocytes. J. Clin. Immunol. *30*, 798–805.

Pircher, H., Bürki, K., Lang, R., Hengartner, H., and Zinkernagel, R.M. (1989). Tolerance induction in double specific T-cell receptor transgenic mice varies with antigen. Nature *342*, 559–561.

Plunkett, F.J., Franzese, O., Belaramani, L.L., Fletcher, J.M., Gilmour, K.C., Sharifi, R., Khan, N., Hislop, A.D., Cara, A., Salmon, M., et al. (2005). The impact of telomere erosion on memory CD8+ T cells in patients with X-linked lymphoproliferative syndrome. Mech. Ageing Dev. *126*, 855–865.

Rao, A., Luo, C., and Hogan, P.G. (1997). Transcription factors of the NFAT family: regulation and function. Annu. Rev. Immunol. *15*, 707–747.

Rao, R.R., Li, Q., Gubbels Bupp, M.R., and Shrikant, P.A. (2012). Transcription factor Foxo1 represses T-bet-mediated effector functions and promotes memory CD8(+) T cell differentiation. Immunity *36*, 374–387.

Richer, M.J., Lang, M.L., and Butler, N.S. (2016). T Cell Fates Zipped Up: How the Bach2 Basic Leucine Zipper Transcriptional Repressor Directs T Cell Differentiation and Function. J. Immunol. *197*, 1009–1015.

Roychoudhuri, R., Clever, D., Li, P., Wakabayashi, Y., Quinn, K.M., Klebanoff, C.A., Ji, Y., Sukumar, M., Eil, R.L., Yu, Z., et al. (2016). BACH2 regulates CD8(+) T cell differentiation by controlling access of AP-1 factors to enhancers. Nat. Immunol. *17*, 851–860.

Sade-Feldman, M., Yizhak, K., Bjorgaard, S.L., Ray, J.P., de Boer, C.G., Jenkins, R.W., Lieb, D.J., Chen, J.H., Frederick, D.T., Barzily-Rokni, M., et al. (2018). Defining T Cell States Associated with Response to Checkpoint Immunotherapy in Melanoma. Cell *175*, 998–1013.e20.

Salih, D.A., and Brunet, A. (2008). FoxO transcription factors in the maintenance of cellular homeostasis during aging. Curr. Opin. Cell Biol. *20*, 126–136.

Sallusto, F., Lenig, D., Förster, R., Lipp, M., and Lanzavecchia, A. (1999). Two subsets of memory T lymphocytes with distinct homing potentials and effector functions. Nature *401*, 708–712.

Shaulian, E., and Karin, M. (2002). AP-1 as a regulator of cell life and death. Nat. Cell Biol. *4*, E131–E136.

Siddiqui, I., Schaeuble, K., Chennupati, V., Fuertes Marraco, S.A., Calderon-Copete, S., Pais Ferreira, D., Carmona, S.J., Scarpellino, L., Gfeller, D., Pradervand, S., et al. (2019). Intratumoral $Tcf1^+PD\text{-}1^+CD8^+$ T Cells with Stem-like Properties Promote Tumor Control in Response to Vaccination and Checkpoint Blockade Immunotherapy. Immunity *50*, 195–211.e10.

Stone, E.L., Pepper, M., Katayama, C.D., Kerdiles, Y.M., Lai, C.Y., Emslie, E., Lin, Y.C., Yang, E., Goldrath, A.W., Li, M.O., et al. (2015). ICOS coreceptor signaling inactivates the transcription factor FOXO1 to promote Tfh cell differentiation. Immunity *42*, 239–251.

Tamahara, T., Ochiai, K., Muto, A., Kato, Y., Sax, N., Matsumoto, M., Koseki, T., and Igarashi, K. (2017). The mTOR-Bach2 Cascade Controls Cell Cycle and Class Switch Recombination during B Cell Differentiation. Mol. Cell. Biol. *37*, e00418-17.

Tejera, M.M., Kim, E.H., Sullivan, J.A., Plisch, E.H., and Suresh, M. (2013). FoxO1 controls effector-to-memory transition and maintenance of functional CD8 T cell memory. J. Immunol. *191*, 187–199.

Trapnell, C., Hendrickson, D.G., Sauvageau, M., Goff, L., Rinn, J.L., and Pachter, L. (2013). Differential analysis of gene regulation at transcript resolution with RNA-seq. Nat. Biotechnol. *31*, 46–53.

Turner, R., and Tjian, R. (1989). Leucine repeats and an adjacent DNA binding domain mediate the formation of functional cFos-cJun heterodimers. Science *243*, 1689–1694.

Utzschneider, D.T., Charmoy, M., Chennupati, V., Pousse, L., Ferreira, D.P., Calderon-Copete, S., Danilo, M., Alfei, F., Hofmann, M., Wieland, D., et al. (2016). T Cell Factor 1-Expressing Memory-like CD8(+) T Cells Sustain the Immune Response to Chronic Viral Infections. Immunity *45*, 415–427.

Utzschneider, D.T., Delpoux, A., Wieland, D., Huang, X., Lai, C.Y., Hofmann, M., Thimme, R., and Hedrick, S.M. (2018). Active Maintenance of T Cell Memory in Acute and Chronic Viral Infection Depends on Continuous Expression of FOXO1. Cell Rep. *22*, 3454–3467.

Vallejo, A.N. (2005). CD28 extinction in human T cells: altered functions and the program of T-cell senescence. Immunol. Rev. *205*, 158–169.

van Dam, H., Duyndam, M., Rottier, R., Bosch, A., de Vries-Smits, L., Herrlich, P., Zantema, A., Angel, P., and van der Eb, A.J. (1993). Heterodimer formation of cJun and ATF-2 is responsible for induction of c-jun by the 243 amino acid adenovirus E1A protein. EMBO J. *12*, 479–487.

Van Der Heide, L.P., Hoekman, M.F., and Smidt, M.P. (2004). The ins and outs of FoxO shuttling: mechanisms of FoxO translocation and transcriptional regulation. Biochem. J. *380*, 297–309.

Weon, B.M., and Je, J.H. (2012). Trends in scale and shape of survival curves. Sci. Rep. *2*, 504.

Wherry, E.J., and Kurachi, M. (2015). Molecular and cellular insights into T cell exhaustion. Nat. Rev. Immunol. *15*, 486–499.

Wherry, E.J., Ha, S.J., Kaech, S.M., Haining, W.N., Sarkar, S., Kalia, V., Subramaniam, S., Blattman, J.N., Barber, D.L., and Ahmed, R. (2007). Molecular signature of CD8+ T cell exhaustion during chronic viral infection. Immunity *27*, 670–684.

Willcox, B.J., Donlon, T.A., He, Q., Chen, R., Grove, J.S., Yano, K., Masaki, K.H., Willcox, D.C., Rodriguez, B., and Curb, J.D. (2008). FOXO3A genotype is strongly associated with human longevity. Proc. Natl. Acad. Sci. USA *105*, 13987–13992.

Wisdom, R. (1999). AP-1: one switch for many signals. Exp. Cell Res. *253*, 180–185.

Wu, T., Ji, Y., Moseman, E.A., Xu, H.C., Manglani, M., Kirby, M., Anderson, S.M., Handon, R., Kenyon, E., Elkahloun, A., et al. (2016). The TCF1-Bcl6 axis counteracts type I interferon to repress exhaustion and maintain T cell stemness. Sci. Immunol. *1*, eaai8593.

Xu, W., and Larbi, A. (2017). Markers of T Cell Senescence in Humans. Int. J. Mol. Sci. *18*, 1742.

Zhang, F., Wang, D.Z., Boothby, M., Penix, L., Flavell, R.A., and Aune, T.M. (1998). Regulation of the activity of IFN-gamma promoter elements during Th cell differentiation. J. Immunol. *161*, 6105–6112.

Zhang, D.J., Wang, Q., Wei, J., Baimukanova, G., Buchholz, F., Stewart, A.F., Mao, X., and Killeen, N. (2005). Selective expression of the Cre recombinase in late-stage thymocytes using the distal promoter of the Lck gene. J. Immunol. *174*, 6725–6731.

Zhang, Y., Liu, T., Meyer, C.A., Eeckhoute, J., Johnson, D.S., Bernstein, B.E., Nusbaum, C., Myers, R.M., Brown, M., Li, W., and Liu, X.S. (2008). Model-based analysis of ChIP-Seq (MACS). Genome Biol. *9*, R137.

Zhang, X., Yalcin, S., Lee, D.F., Yeh, T.Y., Lee, S.M., Su, J., Mungamuri, S.K., Rimmelé, P., Kennedy, M., Sellers, R., et al. (2011). FOXO1 is an essential regulator of pluripotency in human embryonic stem cells. Nat. Cell Biol. *13*, 1092–1099.

Zhang, P.F., Wu, J., Wu, Y., Huang, W., Liu, M., Dong, Z.R., Xu, B.Y., Jin, Y., Wang, F., and Zhang, X.M. (2019). The lncRNA SCARNA2 mediates colorectal cancer chemoresistance through a conserved microRNA-342-3p target sequence. J. Cell. Physiol. *234*, 10157–10165.

Zhou, X., Yu, S., Zhao, D.M., Harty, J.T., Badovinac, V.P., and Xue, H.H. (2010). Differentiation and persistence of memory CD8(+) T cells depend on T cell factor 1. Immunity *33*, 229–240.

STAR★METHODS

KEY RESOURCES TABLE

REAGENT or RESOURCE	SOURCE	IDENTIFIER
Antibodies		
Anti-FOXO1	Cell Signaling Technology	clone C29H4
Anti-FOXO1-phospho-256	Cell Signaling Technology	cat#9461
Anti-FOS	Cell Signaling Technology	clone 9F6
Anti-FOSB	Cell Signaling Technology	clone 5G4
Anti-JunB	Cell Signaling Technology	clone C37F9
Anti-TCF7	Cell Signaling Technology	clone C63D9
Anti-GZMB	BD Biosciences	clone MHGB05
Anti-Ki67	BD Biosciences	clone B56
Anti-IFNg	Thermo Fisher Scientific	clone XMG1.2
Anti-TNFa	Thermo Fisher Scientific	clone MP6-XT22
Anti-IL2	Thermo Fisher Scientific	clone JES6-5H4
Bacterial and virus strains		
LCMV-Armstrong	Expanded in house	Dutko and Oldstone, 1983
Biological samples		
Donor human PBMC	Australian Red Cross / University of Melbourne	https://www.redcross.org.au https://www.unimelb.edu.au
Chemicals, peptides, and recombinant proteins		
JNK inhibitor	Calbiochem	Cat# 420116; (Barr et al., 2002)
Deposited data		
Chip-Seq, ATAC-seq, RNA-seq	https://www.ncbi.nlm.nih.gov/geo/	GEO:GSE163723
Experimental models: organisms/strains		
Foxo1$^{f/f}$	Ronald DePinho, present address, MD Anderson Cancer Center	Paik et al., 2007
Foxo1-AAA	Ming Li, Memorial Sloan Kettering Cancer Center	Ouyang et al., 2012
dLck-Cre	Jackson Laboratories	Zhang et al., 2005
P14 TCR transgenic	Jackson Laboratories	Pircher et al., 1989
C57BL/6J	Jackson Laboratories	strain #000664
Software and algorithms		
HOMER	http://homer.ucsd.edu/homer	Heinz et al., 2010
Galaxy Bioinformatics Server	https://usegalaxy.org	Blankenberg et al., 2010; Giardine et al., 2005; Goecks et al., 2010
Bowtie2	https://usegalaxy.org	Langmead and Salzberg, 2012
MACS2	https://usegalaxy.org	Zhang et al., 2008
Trim Galore	https://usegalaxy.org	http://www.bioinformatics.babraham.ac.uk/projects/trim_galore/
FastQ Groomer	https://usegalaxy.org	Blankenberg et al., 2010
FastQC	https://usegalaxy.org	http://www.bioinformatics.babraham.ac.uk/projects/fastqc/
HISAT2	https://usegalaxy.org	Kim et al., 2015
Cuffdiff2	https://usegalaxy.org	Trapnell et al., 2013

RESOURCE AVAILABILITY

Lead contact

Further information and requests for resources and reagents should be directed to lead contact, Stephen M. Hedrick (shedrick@ucsd.edu).

Materials availability

Reagents are commercially available and/or contacts for all materials are listed in Key resources table.

Data and code availability

Original RNA-seq, ChIP-seq, and ATAC-seq data have been deposited to NCBI GEO/SRA: GSE163723

EXPERIMENTAL MODEL AND SUBJECT DETAILS

Mice and tamoxifen treatment

Mice of various genotypes were congenic with the inbred strain C57BL/6 either by backcrossing or by direct genetic manipulation of C57BL/6 embryos. Host mice for adoptive transfers were either C57BL/6J-CD45.1$^{+/+}$ or C57BL/6J-CD45.1.2. P14$^{+/-}$ TCR-transgenic CD8^{+} T cells specific for LCMV gp33 bound to H2D^{b} (Pircher et al., 1989) are referred to as P14. *Foxo1*$^{f/f}$ mice were crossed to dLck-Cre (B6.Cg-Tg (Lck-icre)3779Nik/J) (Zhang et al., 2005) mice to generate *Foxo1*$^{f/f}$ dLck-Cre$^{+/-}$ mice (*Foxo1*-KO) or *Foxo1*$^{f/f}$ dLck-Cre$^{-/-}$ mice (WT). *Foxo1*-AAA$^{f/f}$ (Ouyang et al., 2012) mice were crossed with dLck-Cre$^{+/-}$ to generate *Foxo1*-AAA mice. For adoptive transfer experiments, these strains were again crossed to P14 mice to generate P14-*Foxo1*-AAA$^{f/f}$ dLck-Cre$^{+/-}$ and P14-*Foxo1*$^{f/f}$ dLck-Cre$^{+/-}$ mice. Mice were maintained in a specific pathogen-free vivarium. All experiments were carried out in accordance to the Institutional Animal Care and Use Committee of University of California, San Diego.

Adoptive transfers and infection

Single-cell suspensions of spleens were homogenized and passed through a 40 μm nylon cell strainer in HBSS (GIBCO) supplemented with 2% fetal bovine serum (FBS), pelleted at 400 x g for 5 minutes, and re-suspended in ACK lysis buffer for five minutes before addition of HBSS/2% FBS media. Adoptive transfers of P14 cells (typically 1 × 10^{4}) were performed via ~200 μL tail vein injection. Acute infections were performed by injection of 2 × 10^{5} pfu LCMV-ARM i.p.

METHOD DETAILS

Immunofluorescent staining and flow cytometry

Surface staining was performed as previously described (Delpoux et al., 2017). Antibody staining was performed with anti-CD4 (RM4-5), anti-CD8α (53-6.7), anti-CD44 (IM7), anti-CD45.1 (A20), anti-CD45.2 (104), anti-CD62L (MEL-14), anti-CD69 (H1.2F3), anti-CD127 (A7R34), anti-KLRG1 (2F1); all from Thermo Fisher or Biolegend. Rabbit anti-mouse TCF7 (C63D9) and FOXO1 (C29H4) were used in both directly-conjugated and secondary staining variations. FOS (9F6), JUNB (C37F9) and FOSB (5G4) antibodies were from Cell Signaling Technologies. Granzyme B (MHGB05) and Ki-67 (B56) antibodies were from BD Biosciences. TBET (4B10) antibody was from BioLegend. Secondary Alexa Fluor 647 donkey anti-rabbit (Invitrogen) was used in some cases as a secondary antibody for detection of FOXO1, FOS, JUNB, FOSB and TCF7 staining. For intracellular staining, the FOXP3 Staining Buffer Set (Thermo Fisher) was used. Immunofluorescence was acquired on a Fortessa or Fortessa X-20 cytometer (BD Biosciences) and analyzed using FlowJo Software (BD Biosciences).

Immunoblotting for FOXO1 and pFOXO-S253

Splenic naive CD8^{+} T cells were purified from mouse spleen with Biolegend naive CD8^{+} isolation kit following the manufacturer's instructions. 1x10^{6} cells were plated *in vitro* with plate-bound anti-CD3 and anti-CD28 (2 μg/ml) for the indicated time. Lysates were prepared in RIPA buffer containing ROCHE cOmplete. CD45.1^{+} cells were positively selected from the splenocytes of LCMV-ARM infected host mice on days 7 and 12 using mouse CD45.1 selection kit from Biolegend, and stimulated *in vitro* using PMA / IONO cocktail (Thermo Fisher) for the indicated time; lysates were prepared as above. 50 μg/sample of total protein were resolved on NuPAGE 4%–12% Bis-Tris pre-cast gels from Thermo Fisher Scientific (NP0321) and transferred to 0.45μm PVDF membrane, incubated overnight at 4°C with primary antibodies. Phospho-FoxO1 (CST; 1:1000; Ser256; cat#9461; note antibody is named for human phospho-site) and FoxO1 (CST; 1:1000; C29H4; cat #2880). beta-tubulin (cat# 05-661; 1:1000; Millipore). Membrane was washed thrice with 1X TBS-Tween20 and incubated with HRP-conjugated secondary antibody (CST, 1:1000 dilution) for 1 hr at room temperature, before chemiluminescent ECL substrate (GE, cat# 34095) imaging on Bio-Rad ChemiDoc and images processed and quantified with ImageJ software.

Cytokine detection

To asses intracellular cytokine production, 2 × 10^{6} splenocytes were cultured for 4h at 37°C with or without PMA/IONO and 10 μg/ml monensin (both Thermo Fisher). Cells were stained for surface markers. Cytofix/Cytoperm Staining Buffer Set (BD Bioscience) was

used for fixation and permeabilization, followed by labeling with specific cytokine antibodies for IFNγ (XMG1.2), TNF (MP6-XT22) and IL-2 (JES6-5H4; all from Thermo Fisher).

In vitro assays

Where indicated, naive $CD8^+$ T cells were purified from total spleen cells with naive $CD8^+$ isolation kit (Stem-Cell or Biolegend), stained with 5 μM of Cell-Trace violet (Thermo Fisher) for 20 min at 37°C followed FBS quench and two washes. $1x10^5$ cells per well were plated in anti-CD3/anti-CD28 each (4 μg/ml) with IL-2 (100U/ml) for 3 days at 37°C. Proliferation index = Log_2 (f), where f = CFSE MFI (in absence of stimulation)/CFSE MFI (in presence of stimulation) (Delpoux et al., 2012). In some wells, JNKi (JNK Inhibitor I, L-Form, Calbiochem) (Barr et al., 2002) was added to 10 μM; JNKi was also added during the 4 hr of cytokine stimulation after the 3 days of culture. For Active Caspase-3 detection, CaspGlow Kit (Thermo fisher) was used per manufacturer's instructions. Briefly, splenocytes were stained for surface markers as described above and cultured at 2×10^6 cells/well in complete media. 1 μL of FITC-DEVD-FMK was added in 300 μL cells. Cells were washed twice and acquired. Anti-activated-caspase3 antibody was used (BD bioscience) with Foxp3 kit was used (Thermo Fisher).

ChIP-seq, RNA-seq, and ATAC-seq

FOXO1 ChIP-seq was performed as before with minor modifications (Lin et al., 2010). Briefly, 3×10^7 T cells were fixed for 5 to 10 minutes at room temp in 1% formaldehyde then resuspended in lysis buffer. Following adaptor ligation, the DNAs were size selected (200-300bp) by 8% PAGE and index primers added by PCR. Samples were purified by 8% PAGE and precipitated with ethanol. Sequencing was performed by the BIOGEM core at UC San Diego using an Illumina HiSeq 2000 sequencer (50 cycles), mapped to mm10 (Bowtie2), and peaks were called with MACS2 and/or HOMER; after manual inspection, artifactual peaks for mir101c, Rn4.5 s, and Pisd-ps3 were removed from the dataset. Peak annotation and motif finding were performed with HOMER (Heinz et al., 2010), and visualized with the UCSC genome browser (Kent et al., 2002).

RNA-seq was performed after cellular isolation by MACS column (naive cells) or FACS (post LCMV-ARM) on total RNA processed using the Illumina Truseq Stranded mRNA library preparation kit followed by single-end 50bp sequencing. Reads were processed on the Galaxy (Blankenberg et al., 2010; Giardine et al., 2005; Goecks et al., 2010) server via: FASTQ Groomer, Trim Galore, FastQC, HISAT2 (Refseq mm10 mapping to known genes first), Cuffdiff2. *mir*, *Snora*, and *Snord* genes were removed before plotting.

Genome-wide measurement of chromatin accessibility and computational alignment of generated data were performed using ATAC-Seq as described (Buenrostro et al., 2013) on 10,000 Naive $CD8^+$ T cells and P14 $KLRG1^{hi}$ or $KLRG1^{low}$ *Foxo1* KO and WT at indicated days LCMV-ARM infection.

Human samples and immunostaining

Following informed consent, peripheral blood mononuclear cells (PBMC) were obtained from healthy donors (recruited from the Australian Red Cross Service). Sero-negative donors for HIV, HCV, HTLV and syphilis were used. The University of Melbourne Human Ethics Committee approved volunteer recruitment and procedures associated. Experiments followed the guidelines set by the Australian NHMRC Code of Practice. Young adult patients were 22-35 years of age, old adults were 60-89 years old. Buffy coats were received from the Australian Red Cross Service (16 – 18h after bleed) and transferred to 50mL tubes. Blood was diluted with RPMI in a 1:1 ratio and mixed. PBMC were isolated using density-gradient centrifugation Ficoll-Paque (GE Healthcare) in 50mL tubes. Frozen PBMCs were thawed in pre-warmed RPMI complete media (RPMI 1640 with 10% FBS, penicillin-streptomycin-glutamine (Thermo Fisher) and 55 μM β-mercaptoethanol (Sigma), washed with RPMI and re-suspended as required for experiments, stained with live/dead discrimination Fixable Viability Dye Near-IR (Thermo Fisher), surface stained for 20 min at 4°C in PBS supplemented with 2% FBS and 2mM EDTA, using the following antibodies: CD3 (UCHT1), CD4 (RPAT4), CD14 (MΦP9), CD45RA (L48) from BD bioscience, and CD8α (RPA-T8), CD19 (HIB19), CD27 (O323) and CD57 (HCD57) from BioLegend. KLRG1 (13F12F2) antibody is from Thermo Fisher, fixed and permeabilized using the Cytofix / Cytoperm kit (BD), or nuclear permeabilization and intracellular staining with FOXP3 transcription factor staining kit (Thermo Fisher). The following intracellular antibodies were used for intracellular or nuclear staining: TCF7 (7F11A10, BioLegend), Rabbit anti-Human FOS (9F6), JUNB (C37F9), FOSB (5G4) and FOXO1 (C29H4) from Cell Signaling Technology. Secondary Alexa Fluor 647 Donkey anti-Rabbit IgG (Invitrogen) was used. Cells were fixed with paraformaldehyde (2% PFA) before sample acquisition.

QUANTIFICATION AND STATISTICAL ANALYSIS

Prism6 software (GraphPad) was used to analyze data by two-tailed unpaired or paired Student's t test when appropriate. * $p < 0.05$; ** $p < 0.01$; *** $p < 0.001$; **** $p < 0.0001$ was considered significant. Data are presented as means ± SEM.